Influence of Cholesterol on Dynamics of Dimyristoylphosphatidylcholine Bilayers as Studied by Deuterium NMR Relaxation

ARTICLE *in* THE JOURNAL OF CHEMICAL PHYSICS · APRIL 1999

Impact Factor: 2.95 · DOI: 10.1063/1.478787

6 AUTHORS, INCLUDING:

Alexander A Nevzorov
North Carolina State University
50 PUBLICATIONS **1,687** CITATIONS
SEE PROFILE

Todd M Alam
Sandia National Laboratories
265 PUBLICATIONS **4,016** CITATIONS
SEE PROFILE

Jaroslav Zajicek
University of Notre Dame
81 PUBLICATIONS **1,809** CITATIONS
SEE PROFILE

Influence of cholesterol on dynamics of dimyristoylphosphatidylcholine bilayers as studied by deuterium NMR relaxation

Theodore P. Trouard,[a] Alexander A. Nevzorov,[b] Todd M. Alam,[c] Constantin Job, Jaroslav Zajicek,[d] and Michael F. Brown[e]
Department of Chemistry, University of Arizona, Tucson, Arizona 85721

(Received 20 May 1998; accepted 2 December 1998)

Investigation of the deuterium (^{2}H) nuclear magnetic resonance (NMR) relaxation rates of lipid bilayers containing cholesterol can yield new insights regarding its role in membrane function and dynamics. Spin-lattice (R_{1Z}) and quadrupolar order (R_{1Q}) ^{2}H NMR relaxation rates were measured at 46.1 and 76.8 MHz for macroscopically oriented bilayers of 1,2-diperdeuteriomyristoyl-*sn*-glycero-3-phosphocholine (DMPC-d_{54}) containing cholesterol (1/1 molar ratio) in the liquid-ordered phase at 40 °C. The data for various segmental positions along the DMPC-d_{54} acyl chain were simultaneously fitted to a composite membrane deformation model, including fast segmental motions which preaverage the coupling tensor along the lipid acyl chain, slow molecular reorientations, and small-amplitude collective fluctuations. In contrast to pure DMPC-d_{54} in the liquid-crystalline (L_α) phase, for the DMPC-d_{54}:cholesterol (1/1) system a linear square-law functional dependence of the relaxation rates on the order parameter (quadrupolar splitting) does not appear evident. Moreover, for acyl segments closer to the top of the chain, the angular anisotropy of the ^{2}H R_{1Z} and R_{1Q} relaxation rates is more pronounced than toward the chain terminus. The residual (preaveraged) coupling tensor has its greatest effective asymmetry parameter near the polar groups, decreasing for the groups closest to the end of the chain. The results suggest that axial rotations of the phospholipid molecules occur at a somewhat higher rate than in pure bilayers, as a consequence of the higher ordering and reduction of chain entanglement. On the other hand, the rigid cholesterol molecule appears to undergo somewhat slower axial rotation, possibly due to its noncylindrical shape. Collective motions are found to be less predominant in the case of DMPC-d_{54}:cholesterol than for pure DMPC-d_{54}, which may indicate an increased dynamical rigidity of lipid bilayers containing cholesterol versus pure lipid systems. © *1999 American Institute of Physics.* [S0021-9606(99)00510-3]

I. INTRODUCTION

Deuterium (^{2}H) nuclear spin relaxation of lipid bilayers is sensitive to the rates and amplitudes of various motions of lipid molecules, and constitutes a powerful method for studying the dynamics of these important biological liquid crystalline assemblies.[1,2] Comparison of the ^{2}H nuclear magnetic resonance (NMR) relaxation rates of bilayers containing cholesterol to pure lipid bilayers can help investigate its role in membrane function and dynamics.[3–10] Cholesterol is a common component of biological membranes[11] and is implicated in cardiovascular diseases.[12] In addition, its inclusion into reconstituted phosphatidylcholine vesicles has been observed to alter the activity of the visual protein rhodopsin.[13,14] A significant effort has been made to understand the effect of cholesterol on the biophysical properties of lipid bilayers.[9–11,15–22] The inclusion of cholesterol in a lipid bilayer has been shown to yield a liquid-ordered phase[20,23] and to increase the orientational order of the acyl chains,[3,24–30] accompanied by an increase in the average thickness of the hydrocarbon region.[31–33] Micromechanical studies of unilamellar vesicles have also revealed an increase in the bulk bending modulus of bilayers containing cholesterol.[34,35] A decrease in bilayer permeability has been associated with the presence of cholesterol in liposomes of polyunsaturated lecithin.[36] In spite of these effects, lipid molecules in bilayers containing cholesterol still experience significant axial and lateral diffusion similar to pure lipid bilayers.[21,37–43]

It follows that cholesterol-rich lipid bilayers in the liquid-ordered phase provide an interesting system of biological soft matter,[7,11] the dynamical and equilibrium properties of which can be effectively studied by deuterium (^{2}H) NMR techniques. Quantitative information about the effect of cholesterol on lipid dynamics, including the degree of molecular ordering, reorientation rates, and the bilayer elastic constants, can be obtained from the analysis of nuclear spin relaxation rates by invoking specific models for various motions of membrane constituents, and by using NMR relaxation theory.[8,10] The validity of the interpretation of the ex-

[a]Present address: Department of Radiology, University of Arizona, Tucson, Arizona 85724.
[b]Present address: Department of Chemistry and Chemical Biology, Cornell University, Ithaca, New York 14853.
[c]Present address: Sandia National Laboratories, Albuquerque, New Mexico 87185.
[d]Present address: Department of Chemistry and Biochemistry, University of Notre Dame, Notre Dame, Indiana 46556.
[e]Additional address: Division of Physical Chemistry 1, Center for Chemistry and Chemical Engineering, Lund University, S-221 00 Lund, Sweden.

perimental results depends on the relevance of the motional model which is used to fit the data. Several models have been proposed to describe the dynamics of lipid molecules within the bilayer, including fast segmental reorientations,[44–47] molecular diffusion,[47–49] and collective fluctuations.[47,50–52] In addition, numerical methods can be invoked to simulate the observed relaxation rates by solving the Liouville-von Neumann equation.[53–56] Analysis of a broad range of experimental relaxation data as a function of frequency, sample orientation, and temperature has suggested that consideration of faster segmental motions, noncollective molecular reorientations, and collective membrane excitations is needed to account for the ^{2}H NMR relaxation rates of pure lipid bilayers in the fluid phase.[57–59]

As a further step beyond investigating pure lipid membranes, one can utilize ^{2}H NMR relaxation to analyze how the dynamical properties of a bilayer are influenced by the presence of other membrane constituents such as cholesterol. Little effect of cholesterol on the ^{2}H NMR quadrupolar splittings and relaxation rates of the headgroup and glycerol backbone region of phospholipids has been observed in bilayer mixtures.[16,60–62] However, in contrast to pure phospholipid bilayers,[44,62–65] a striking angular anisotropy of the spin-lattice relaxation (R_{1Z}) is found for both the lipid acyl chains[8,62,66] and the cholesterol molecule itself in oriented systems.[67,68] The results show that at a single magnetic field strength, jump models,[66,68] segmental or molecular diffusion models,[8] or a treatment based on solution of the Liouville-von Neumann equation[9] can all describe the ^{2}H NMR relaxation rates as a function of sample orientation. Therefore, analysis of a broader range of experimental NMR relaxation data as a function of more than one variable, including the ^{2}H NMR frequency and segmental position in the lipid acyl chains, is needed to further test various dynamical models for membrane constituents,[10,59] and to establish the correspondence to biophysical properties.

In the present work, ^{2}H spin-lattice (R_{1Z}) and quadrupolar order (R_{1Q}) relaxation rates have been measured at two different frequencies (46.1 and 76.8 MHz) for macroscopically oriented bilayers of 1,2-diperdeuteriomyristoyl-*sn*-glycero-3-phosphocholine (DMPC-d_{54}) containing cholesterol (1/1 molar ratio) in the liquid-ordered phase at 40 °C. The experimental data for the entire perdeuterated lipid acyl chain have been simultaneously analyzed in terms of a composite membrane deformation model,[59] including a variable residual coupling tensor due to fast segmental motions that is further modulated by slower collective excitations and molecular reorientations. The model gives similar results to the numerical solution of the stochastic Liouville-von Neumann equation,[9] but yields an expression for the spectral density in closed form. Finally, the dynamical structure of the mixed bilayers containing cholesterol is discussed within the framework of the model.

II. GENERAL THEORETICAL BACKGROUND

Using NMR relaxation theory,[1,69,70] the spin-lattice relaxation rate R_{1Z} can be expressed as a linear combination of spectral densities of motion $J_m(\omega,\beta_{DL})$ in the following manner:[71]

$$R_{1Z}(^2\mathrm{H}) = \tfrac{3}{4}\pi^2\chi_Q^2[J_1(\omega_\mathrm{D},\beta_{DL}) + 4J_2(2\omega_\mathrm{D},\beta_{DL})]. \tag{2.1}$$

The decay of the quadrupolar order R_{1Q} can be similarly calculated as[71]

$$R_{1Q}(^2\mathrm{H}) = \tfrac{9}{4}\pi^2\chi_Q^2 J_1(\omega_\mathrm{D},\beta_{DL}). \tag{2.2}$$

Here $\chi_Q = e^2qQ/h = 170$ kHz is the static quadrupolar coupling constant, ω_D is the deuteron Larmor frequency, and β_{DL} defines the macroscopic orientation of the bilayer normal (director frame) with respect to the magnetic field (laboratory frame). Note that in general the spectral densities of motion, and therefore the spin relaxation rates in Eqs. (2.1) and (2.2), contain not only the dependence on the deuteron Larmor frequency (ω_D), but also the dependence on the orientation of the bilayer ($\beta_{DL} \equiv \theta$). The spectral densities of motion $J_m(\omega,\beta_{DL})$, where $m = 0$, 1, and 2, are Fourier transforms of the corresponding correlation functions $G_m(\tau,\beta_{DL})$ which describe the time-dependent orientation of the irreducible components of the electric field gradient (EFG)[72] tensor with respect to the external magnetic field (laboratory frame),

$$J_m(\omega,\beta_{DL}) = \int_{-\infty}^{+\infty} G_m(\tau,\beta_{DL}) e^{-i\omega\tau} d\tau. \tag{2.3}$$

If the static EFG tensor is assumed to be axially symmetric for saturated lipid chains, the laboratory-frame correlation functions are given in terms of the elements of the second-rank Wigner rotation matrix $\mathbf{D}^{(2)}(\Omega_{PL})$ by

$$G_m(\tau,\beta_{DL}) = \langle [D_{0m}^{(2)}(\Omega_{PL};t+\tau) - \langle D_{0m}^{(2)}(\Omega_{PL})\rangle]^* \times [D_{0m}^{(2)}(\Omega_{PL};t) - \langle D_{0m}^{(2)}(\Omega_{PL})\rangle]\rangle. \tag{2.4}$$

The Euler angles Ω_{PL} in the above expression describe the overall transformation of the principal axis system (PAS) of the EFG tensor to the laboratory frame. By applying the well-known closure property of the Wigner rotation matrices,[73] for the case of continuous axially symmetric motions, one can separate the frequency dependence from the orientation dependence in the correlation function to yield[49,74]

$$\begin{aligned} G_m(\tau,\beta_{DL}) = {} & |D_{0m}^{(2)}(\Omega_{DL})|^2 G_0^{\mathrm{dir}}(\tau) \\ & + [|D_{-1m}^{(2)}(\Omega_{DL})|^2 + |D_{1m}^{(2)}(\Omega_{DL})|^2] G_1^{\mathrm{dir}}(\tau) \\ & + [|D_{-2m}^{(2)}(\Omega_{DL})|^2 + |D_{2m}^{(2)}(\Omega_{DL})|^2] G_2^{\mathrm{dir}}(\tau). \end{aligned} \tag{2.5}$$

Here the Euler angles Ω_{DL} correspond to the orientation of the sample as a whole relative to the main magnetic field (laboratory frame). All dynamical information is therefore contained in the director-frame correlation functions, which are defined as

$$G_p^{\mathrm{dir}}(\tau) = \langle [D_{0p}^{(2)}(\Omega_{PD};t+\tau) - \langle D_{0p}^{(2)}(\Omega_{PD})\rangle]^* \times [D_{0p}^{(2)}(\Omega_{PD};t) - \langle D_{0p}^{(2)}(\Omega_{PD})\rangle]\rangle, \tag{2.6}$$

where $p = 0$, 1, and 2, and the angles Ω_{PD} describe the orientation of the PAS relative to the average normal to the bilayer surface (director). In order to analyze the experimen-

tal R_{1Z} and R_{1Q} angular anisotropies at different frequencies, as given by Eqs. (2.1) and (2.2), the functional form of the director-frame correlation functions $G_P^{\mathrm{dir}}(\tau)$ must be derived from a specific physical model describing fluctuations of the coupling tensor associated with a given C–^{2}H bond (segment).

III. COMPOSITE MEMBRANE DEFORMATION MODEL INCLUDING RESIDUAL COUPLING TENSOR

As a means of separating various motions, including fast segmental motions, slower molecular reorientations, and collective fluctuations in Eq. (2.6), one can further apply the convenient closure property of the Wigner matrix elements $D_{0p}^{(2)}(\Omega_{PD})$, that is[59]

$$D_{0p}^{(2)}(\Omega_{PD};t)=\sum_r \sum_q \sum_n D_{0r}^{(2)}(\Omega_{PI};t)D_{rq}^{(2)}(\Omega_{IM}) \times D_{qn}^{(2)}(\Omega_{MN};t)D_{np}^{(2)}(\Omega_{ND};t). \tag{3.1}$$

In the above expression, the first transformation is from the principal axis system (PAS) of the static electric field gradient tensor to the intermediate frame associated with the PAS of the residual coupling tensor, which is given by the Euler angles $\Omega_{PI}(t)$ and arises from segmental reorientations; the second rotation is given by Ω_{IM} and represents the fixed transformation from the intermediate frame to the frame associated with the lipid molecule; the third rotation $\Omega_{MN}(t)$ describes diffusive reorientations of the lipid molecules; and finally the fourth transformation pertains to the collective fluctuations of the instantaneous membrane normal with respect to the average membrane normal (director) as given by the angles $\Omega_{ND}(t)$.

Assuming that the segmental reorientations are fast on the ^{2}H NMR time scale, one can average over their motional amplitudes, and introduce a residual coupling tensor[75] with the components[65]

$$\chi_Q^{\mathrm{eff}}=\chi_Q\langle D_{00}^{(2)}(\Omega_{PI})\rangle\equiv\chi_Q S_f^{(2)}, \tag{3.2a}$$

$$\eta_Q^{\mathrm{eff}}\equiv-\sqrt{6}\frac{\langle D_{0\pm2}^{(2)}(\Omega_{PI})\rangle}{\langle D_{00}^{(2)}(\Omega_{PI})\rangle}=-\frac{3}{2}\frac{\langle \sin^2\beta_{PI}\cos(2\gamma_{PI})\rangle}{S_f^{(2)}}. \tag{3.2b}$$

Note that the intermediate frame is chosen so that the residual coupling tensor is diagonal, yielding the following expression for the director-frame correlation functions,

$$G_p^{\mathrm{dir}}(\tau)=S_f^{(2)^2}\sum_{q=-2}^{2}\sum_{n=-2}^{2}\left|D_{0q}^{(2)}(\Omega_{IM})-\frac{\eta_Q^{\mathrm{eff}}}{\sqrt{6}}[D_{-2q}^{(2)}(\Omega_{IM})+D_{2q}^{(2)}(\Omega_{IM})]\right|^2\{[G_{qn}^{\mathrm{mol}}(\tau)+S_s^{(2)^2}\delta_{0q}\delta_{0n}]G_{np}^{\mathrm{col}}(\tau)-S_s^{(2)^2}\delta_{0q}\delta_{0n}\delta_{0p}\}. \tag{3.3}$$

It follows from Eq. (3.3) that even though the static coupling tensor is symmetric, fast segmental motions may result in an asymmetric residual coupling tensor having a variable orientation of the z-axis of its principal axis system as given by the Euler angles $\Omega_{IM}\equiv(\alpha_{IM},\beta_{IM},0)$. The overall order parameter S_{CD} which is experimentally determined from the quadrupolar splitting, viz. $\Delta\nu_Q=\frac{3}{2}\chi_Q S_{\mathrm{CD}}$, can then be expressed in terms of the fast and slow order parameters $S_f^{(2)}$ and $S_s^{(2)}$ in the following manner:[65]

$$S_{\mathrm{CD}}=S_f^{(2)}\left\{D_{00}^{(2)}(\Omega_{IM})-\frac{\eta_Q^{\mathrm{eff}}}{\sqrt{6}}[D_{-20}^{(2)}(\Omega_{IM})+D_{20}^{(2)}(\Omega_{IM})]\right\}S_s^{(2)}. \tag{3.4}$$

Here $S_f^{(2)}=\langle D_{00}^{(2)}(\Omega_{PI})\rangle$ and $S_s^{(2)}=\langle D_{00}^{(2)}(\Omega_{MN})\rangle\langle D_{00}^{(2)}(\Omega_{ND})\rangle\approx\langle D_{00}^{(2)}(\Omega_{MN})\rangle$ for small-amplitude director fluctuations.

In terms of a strong-collisional approximation,[76] the director-frame correlation functions for noncollective molecular motions are given by[47]

$$G_{qn}^{\mathrm{mol}}(\tau)=[\langle|D_{qn}^{(2)}(\Omega_{MN})|^2\rangle-|\langle D_{qn}^{(2)}(\Omega_{MN})\rangle|^2\delta_{q0}\delta_{n0}]e^{-\tau/\tau_{qn}}. \tag{3.5}$$

Following the classic work of Nordio and Segre,[76] the correlation times for various reorientational modes τ_{qn} are obtained from the theory of anisotropic rotational diffusion in the presence of a potential of mean torque,[48,65,76] $U(\beta_{MN})=-\lambda_j P_j(\cos\beta_{MN})$, where $P_j(\cos\beta_{MN})$ is a Legendre polynomial of rank $j=1,2$. If $j=1$, the parity of the potential is odd,[8,49], whereas if $j=2$ the parity is even.[47] The correlation times τ_{qn} are then calculated as[48]

$$\frac{1}{\tau_{qn}}=\frac{\mu_{qn}}{\langle|D_{qn}^{(2)}(\Omega_{MD})|^2\rangle-|\langle D_{qn}^{(2)}(\Omega_{MD})\rangle|^2\delta_{q0}\delta_{n0}}D_\perp+(D_\parallel-D_\perp)n^2, \tag{3.6}$$

where $D_\parallel$ and $D_\perp$ are diffusion coefficients for the axial and transverse rotations with respect to the long molecular axis, respectively. The moments μ_{qn} are evaluated in terms of the order parameters $\langle D_{00}^{(j)}(\Omega_{MD})\rangle$, where $j=1$, 2, 3, and 4, by using the Clebsch-Gordan series expansion as discussed by

Trouard *et al.*[65] The latter can be found from the Boltzmann distribution in terms of the potential of mean torque $U(\beta_{MD})$, namely

$$\langle D_{00}^{(j)}(\Omega_{MD})\rangle = \frac{\int_0^{\pi} D_{00}^{(j)}(\Omega_{MD})\exp[-U(\beta_{MD})/kT]\sin\beta_{MD}d\beta_{MD}}{\int_0^{\pi}\exp[-U(\beta_{MD})/kT]\sin\beta_{MD}d\beta_{MD}}. \tag{3.7}$$

Note that in the simplest case of a strong-collisional symmetric top approximation, Eq. (3.6) leads to $1/\tau_{qn}=6D_{\perp}+(D_{\parallel}-D_{\perp})n^2$, and hence the rotational diffusion is described in terms of $D_{\parallel}$ and $D_{\perp}$ by three correlation times.[47]

Next we consider the contribution from collective order-director fluctuations (ODF). Given that the collective fluctuations are formulated as three-dimensional thermal excitations,[77] and considering only the director fluctuations to linear order[47,78,79] in $\beta_{ND}(t)$, one can further write that

$$G_{00}^{\mathrm{col}}(\tau)=G_{11}^{\mathrm{col}}(\tau)=G_{22}^{\mathrm{col}}(\tau)=1, \tag{3.8a}$$

$$G_{12}^{\mathrm{col}}(\tau)=G_{21}^{\mathrm{col}}(\tau)=\langle\beta_{ND}(t+\tau)\beta_{ND}(t)\rangle=\frac{5}{3\sqrt{2\pi}}\frac{D}{\sqrt{\tau}}, \tag{3.8b}$$

$$G_{01}^{\mathrm{col}}(\tau)=G_{\pm 10}^{\mathrm{col}}(\tau)=\frac{5}{2\sqrt{2\pi}}\frac{D}{\sqrt{\tau}}. \tag{3.8c}$$

Here the constant factor D is a function of the elasticity, viscosity, and temperature of the bilayer,[47,79] and all other correlation functions for collective motions are zero in this order.

The final expression for the spectral density of motion is then obtained by Fourier transforming the expression for the correlation function, Eqs. (2.5) and (3.3), and can be recast in the following general form,[59,80,81] herein referred to as the composite membrane deformation model:[59]

$$J_m(\omega,\beta_{DL})=J_m^{\mathrm{mol}}(\omega,\beta_{DL})+J_m^{\mathrm{col}}(\omega,\beta_{DL})+J_m^{\text{mol-col}}(\omega,\beta_{DL}). \tag{3.9}$$

In the above expression, the molecular spectral densities are given by[47,52,65]

$$J_m^{\mathrm{mol}}(\omega,\beta_{DL})=S_f^{(2)^2}\sum_{q=-2}^{2}\sum_{n=-2}^{2}\left|D_{0q}^{(2)}(\Omega_{IM})-\frac{\eta_Q^{\mathrm{eff}}}{\sqrt{6}}[D_{-2q}^{(2)}(\Omega_{IM})+D_{2q}^{(2)}(\Omega_{IM})]\right|^2$$
$$\times[\langle|D_{qn}^{(2)}(\Omega_{MD})|^2\rangle-|\langle D_{00}^{(2)}(\Omega_{MD})\rangle|^2\delta_{q0}\delta_{n0}]j_{qn}^{(2)}(\Omega_{MD};\omega)|D_{nm}^{(2)}(\Omega_{DL})|^2, \tag{3.10}$$

where $j_{qn}^{(2)}(\Omega_{MD};\omega)$ are Lorentzian reduced spectral densities with correlation times τ_{qn} which can be determined from Eq. (3.6). The 3D collective spectral densities of motion can be written as[47,52,65]

$$J_m^{\mathrm{col}}(\omega,\beta_{DL})=\tfrac{5}{2}S_f^{(2)^2}D\omega^{-1/2}[|D_{-1m}^{(2)}(\Omega_{DL})|^2+|D_{1m}^{(2)}(\Omega_{DL})|^2]. \tag{3.11}$$

Finally, the cross term $J_m^{\text{mol-col}}(\omega,\beta_{DL})$ can be calculated to yield

$$J_m^{\text{mol-col}}(\omega,\beta_{DL})=S_f^{(2)^2}\sum_{q=-2}^{2}\left|D_{0q}^{(2)}(\Omega_{IM})-\frac{\eta_Q^{\mathrm{eff}}}{\sqrt{6}}[D_{-2q}^{(2)}(\Omega_{IM})+D_{2q}^{(2)}(\Omega_{IM})]\right|^2\Bigg\{J_{q1}^{\text{mol-col}}(\omega)[3|D_{0m}^{(2)}(\Omega_{DL})|^2$$
$$+|D_{-2m}^{(2)}(\Omega_{DL})|^2+|D_{2m}^{(2)}(\Omega_{DL})|^2]+\left[\frac{3}{2}J_{q0}^{\text{mol-col}}(\omega)+J_{q2}^{\text{mol-col}}(\omega)\right][|D_{-1m}^{(2)}(\Omega_{DL})|^2+|D_{1m}^{(2)}(\Omega_{DL})|^2]\Bigg\}. \tag{3.12}$$

In the linear-order approximation for director amplitudes, the individual terms $J_{qn}^{\text{mol-col}}(\omega)$ comprise Fourier transforms of the products of the correlation functions $G_{qn}^{\mathrm{mol}}(\tau)$ which describe the various modes of molecular reorientations q and n, cf. Eq. (3.5), and the correlation functions for collective motions $G_{qn}^{\mathrm{col}}(\tau)$ as given by Eqs. (3.8a)–(3.8c). After calculating the Fourier integrals, one obtains[59]

$$J_{qn}^{\text{mol-col}}(\omega)=[\langle|D_{qn}^{(2)}(\Omega_{MN})|^2\rangle-|\langle D_{00}^{(2)}(\Omega_{MN})\rangle|^2\delta_{q0}\delta_{n0}]\frac{5}{3}D\sqrt{\frac{\tau_{qn}[1+\sqrt{1+(\omega\tau_{qn})^2}]}{1+(\omega\tau_{qn})^2}}, \tag{3.13}$$

for all q and n of Eq. (3.12).

Thus as given by the composite membrane deformation model,[59] the frequency dependence of the relaxation arises from slower molecular motions and collective fluctuations of the bilayer,[47] as described by the sum of their corresponding spectral densities and a cross term. On the other hand, fast segmental reorientations yield a residual coupling tensor with variable components χ_Q^{eff} and η_Q^{eff} along the lipid acyl chain.[75]

IV. EXPERIMENTAL PROCEDURES

A. Lipid synthesis and sample preparation

1,2-diperdeuteriomyristoyl-*sn*-glycero-3-phosphocholine (DMPC-d_{54}) was synthesized from the anhydride of its perdeuterated acid and the cadmium adduct of *sn*-glycero-3-phosphocholine.[82,83] The purity of the lipid was checked by thin layer chromatography in $CHCl_3$:MeOH:H_2O (65/35/5) followed by charring with 40% H_2SO_4. Choles-

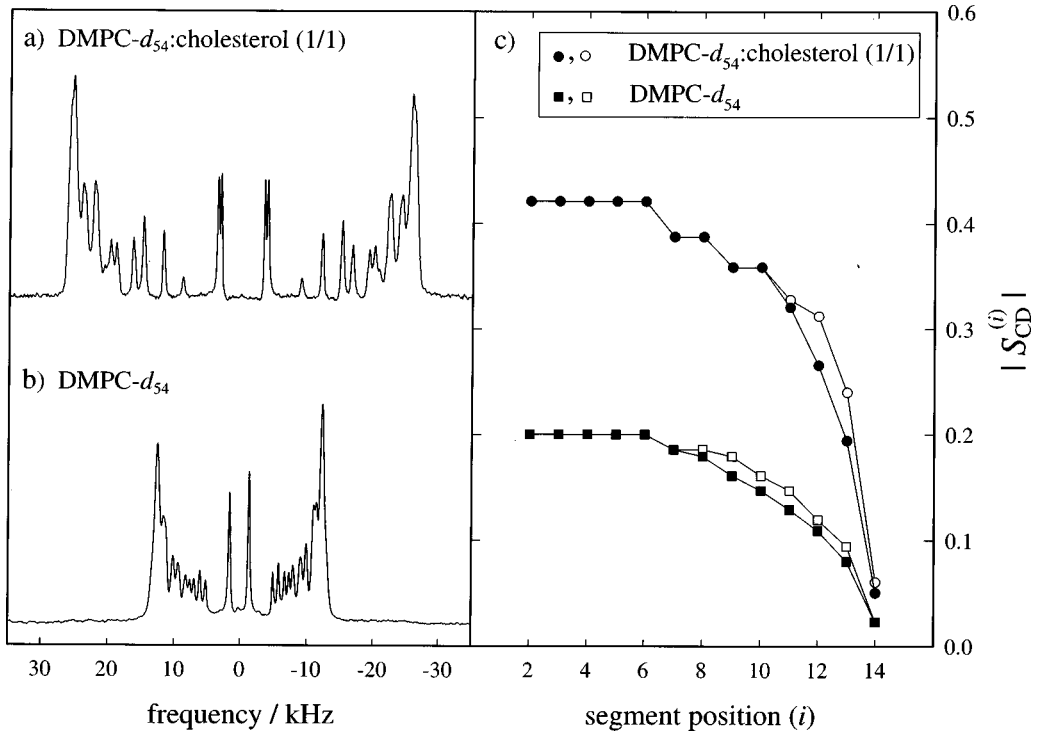

FIG. 1. Comparison of ^{2}H NMR spectra at 46.1 MHz and derived order parameter profiles of lipid bilayers showing the influence of cholesterol at $T = 40$ °C. (a) Deuterium NMR spectrum of macroscopically oriented DMPC-d_{54}:cholesterol (1/1) bilayers having perdeuterated acyl chains in the liquid-ordered phase; and (b) ^{2}H NMR spectrum of bilayers of DMPC-d_{54} in the liquid-crystalline (L_α) phase. In each case the sample tilt $\theta \equiv \beta_{DL} = 90°$. A greater degree of ordering is observed in the case of DMPC-d_{54}:cholesterol versus pure DMPC-d_{54} bilayers, as evinced by the larger ^{2}H NMR quadrupolar splittings in the former case. (c) Profiles of the order parameter $|S_{CD}^{(i)}|$ as a function of acyl segment position (i) for both the sn-1 (●) and sn-2 (○) acyl chains of DMPC-d_{54}:cholesterol (1/1) in comparison with the sn-1 (■) and sn-2 (□) chains of pure DMPC-d_{54} bilayers. The assignments of the various quadrupolar splittings are given in Tables I and II.

terol (99+ %) was obtained from Sigma (St. Louis, MO) and used without further purification. Lipid:cholesterol samples for ^{2}H NMR spectroscopy were prepared by first dissolving appropriate amounts of the two components in chloroform, followed by lyophilization from cyclohexane to form a dry powder.[84] The resulting powder was then hydrated in Tris buffer (about 70 wt. % buffer), containing 1 mM of ethylenediaminetetraacetic acid at pH = 7.3, and a macroscopically oriented lipid sample was prepared for NMR spectroscopy as previously described.[61,65]

B. Nuclear magnetic resonance spectroscopy

Deuterium NMR spectroscopy was performed using two spectrometers having superconducting magnets of 7.06 and 11.05 Tesla with ^{2}H Larmor frequencies of 46.1 and 76.8 MHz, respectively.[84] An external 1 kW radio frequency amplifier (Henry Radio Tempo 2006-A, Los Angeles, CA) and a home-built, high-power deuterium probe, having a transverse solenoid coil (8 mm diameter) and using Polyflon Corporation (New Rochelle, NY) capacitors were employed to obtain $\pi/2$ pulse widths of 2.1 and 3.2 μs for 46.1 and 76.8 MHz, respectively. All ^{2}H NMR spectra were recorded by using quadrature detection with a 2 μs dwell time (±250 kHz spectral width). The sample temperature was maintained at 40 °C by passing heated air over the sample in a Dewared glass chamber enclosing the radio frequency coil. Values of the carbon-deuterium bond order parameter $S_{CD}^{(i)}$ and macroscopic bilayer orientation θ were obtained by fitting simultaneously the observed quadrupolar splittings $\Delta\nu_Q^{(i)}$ at various sample orientations to the expression $\Delta\nu_Q^{(i)} = \frac{3}{2} S_{CD}^{(i)} P_2(\cos\theta)$, where $P_2(\cos\theta)$ is a second-rank Legendre polynomial. Initial estimates of θ and $S_{CD}^{(i)}$ were obtained by multiple measurements near the $\theta = 0$ and 90° orientations, and were further refined by the above fitting procedure, which enabled an accurate determination of the sample tilt angle to within ±1°.

Spin-lattice relaxation (R_{1Z}) rates were determined using an inversion recovery pulse sequence, $(\pi)_\phi - t_1 - (\pi/2)_\phi - \tau_1 - (\pi/2)_{\phi\pm 90} - \tau_2 -$ acquire, with a 32-step phase cycling routine.[85] Twenty values of the delay time t_1 ranged from 2 ms to 1.5 s, and the time between successive experiments was 1.5 s. The decay of the quadrupolar order (R_{1Q}) was determined using a modified version[8] of the Jeener-Broekaert pulse sequence,[86] $(\pi/2)_\phi - 2\tau_1 - (3\pi/8)_{\phi-90} - 2\tau_1 - (\pi/4)_{\phi+90} - \tau_1 - (\pi/4)_{\phi+90} - t_1 - (\pi/4)_\phi - \tau_2 - (\pi/2)_\phi - \tau_2 -$ acquire. The broadband Jeener-Broekaert pulse sequence creates quadrupolar order over a broad range near the carrier frequency, which is ideally suited for ^{2}H NMR spectra with multiple quadrupolar splittings.[8,87] A $\pi/2$ refocusing pulse was added[8,88] to the above sequence and phase cycling[85] was employed. The measurements of the R_{1Q} relaxation rates for pure DMPC-d_{54} bilayers using the broadband[86] and the standard[85] Jeener-Broekaert pulse sequences yielded identical results.[84]

TABLE I. Deuterium spin-lattice (R_{1Z}) and quadrupolar order (R_{1Q}) relaxation rates for *sn*-1 and *sn*-2 acyl chains of DMPC-d_{54}:cholesterol (1/1) in the liquid-ordered phase at 40 °C and 46.1 MHz.

Reso-	Acyl chain segment[a]			$R_{1Z}(\theta)/s^{-1}$						$R_{1Q}(\theta)/s^{-1}$					
nance	*sn*-1	*sn*-2	$\lvert S_{CD}\rvert$	$\theta=0°$	13°	30°	68°	80°	90°	0°	13°	30°	68°	80°	90°
A	2–6	3–6	0.4330	38.2	37.6	32.7	19.7	17.6	17.0	8.8	9.2	12.0	19.8	19.2	21.0
				±2.2	±1.6	±1.6	±1.4	±0.5	±0.8	±0.5	±0.3	±0.5	±1.0	±1.1	±1.5
B	7,8	7,8	0.4094	30.0	29.3	27.8	19.0	16.1	15.6	9.7	9.4	13.3	16.9	16.5	15.3
				±3.6	±2.6	±2.6	±1.6	±1.1	±1.3	±1.8	±0.7	±1.7	±1.7	±1.5	±1.3
C	9,10	9,10	0.3796	23.7	24.1	25.1	18.6	16.6	17.1	11.3	11.3	13.9	16.1	16.7	14.9
				±1.2	±1.0	±1.0	±0.4	±0.2	±0.4	±0.8	±0.4	±0.7	±1.2	±1.6	±1.3
D	11	⋯	0.3380	17.0	16.1	15.0	13.6	14.8	14.3	8.8	7.9	10.2	9.2	10.0	11.4
				±0.5	±0.4	±0.3	±0.3	±0.3	±0.8	±0.4	±0.3	±1.8	±1.0	±0.8	±1.2
E	⋯	12	0.3240	13.1	13.0	13.2	10.6	11.5	11.2	5.3	6.8	9.6	7.9	8.8	7.0
				±0.3	±0.3	±0.2	±0.3	±0.3	±0.6	±0.2	±0.8	±1.7	±0.3	±1.2	±1.2
F	12	⋯	0.2814	9.1	9.6	10.8	10.4	10.6	10.2	7.7	8.1	9.5	7.1	6.4	7.5
				±0.2	±0.2	±0.3	±0.2	±0.2	±0.4	±0.6	±0.4	±0.9	±0.6	±1.1	±0.2
G	⋯	13,2a	0.2551	12.4	11.0	11.5	11.0	11.7	13.1	8.7	10.8	9.9	7.5	7.8	7.4
				±0.6	±0.5	±0.5	±0.6	±0.4	±1.0	±1.1	±0.6	±0.6	±0.4	±0.7	±0.8
H	13	⋯	0.2051	7.9	8.3	7.7	8.3	8.7	8.8	9.3	9.1	6.9	4.5	5.2	4.2
				±0.9	±1.1	±0.7	±1.0	±1.1	±0.9	±1.2	±0.5	±0.3	±0.3	±0.2	±0.3
I	14	⋯	0.0635	2.8	2.8	3.3	3.7	4.0	4.0	4.2	3.2	3.2	2.2	1.9	1.9
				±0.4	±0.2	±0.4	±0.5	±0.4	±0.3	±0.3	±0.2	±0.4	±0.3	±0.2	±0.2

[a]Spectral assignments are from Ref. 84.

V. RESULTS

A representative ^{2}H NMR spectrum of macroscopically oriented bilayers of DMPC-d_{54} containing cholesterol (1/1 molar ratio) measured at 46.1 MHz is shown in part (a) of Fig. 1. The angle $\theta(\equiv\beta_{DL})$ between the bilayer normal and external magnetic field was set at 90°. This spectrum can be compared with that of pure DMPC-d_{54} bilayers,[59] which is shown in part (b) of Fig. 1. Several model-independent observations of a general nature can be made from analysis of the ^{2}H NMR data of DMPC-d_{54} bilayers containing cholesterol versus those of pure DMPC-d_{54} bilayers. The first observation regarding the effect of cholesterol on lipid bilayers is that the ^{2}H NMR quadrupolar splittings in the DMPC-d_{54}:cholesterol spectrum are larger, which is due to a decreased chain mobility, yielding a greater ordering of the acyl chain segments and thereby accounting for the well-known condensing effect of cholesterol.[24,25,89] The inequivalence of the *sn*-1 and *sn*-2 acyl chains can be seen from the smallest splittings corresponding to the acyl terminal methyl groups in the DMPC-d_{54}:cholesterol spectrum, which yield single peaks in the case of pure DMPC-d_{54} bilayers. Part (c) of Fig. 1 shows profiles of the carbon-deuterium bond order parameters $\lvert S_{CD}^{(i)}\rvert$ obtained from the relation $\Delta\nu_Q^{(i)} = \frac{3}{2}S_{CD}^{(i)}P_2(\cos\theta)$, which are, in general, a measure of the average angular fluctuations of the segments about the all-*trans* acyl chain conformation as obtained from the quadrupolar splittings. The order parameters for the cholesterol-containing DMPC-d_{54} bilayers are compared to those for pure DMPC-d_{54}, and are consistent with previous work.[25,83] As can be seen from part (c) of Fig. 1, in the case of DMPC-d_{54}:cholesterol bilayers, the C2–C6 acyl chain segments yield the largest quadrupolar splitting (the plateau region), corresponding to an order parameter of $\lvert S_{CD}\rvert = 0.42$ which is near the limiting value of $\lvert S_{CD}\rvert = 1/2$ for an all-trans chain undergoing axial rotation about its long axis. On the other hand, the order parameters for pure DMPC-d_{54} are nearly twofold smaller. The spectral assignments of the quadrupolar splittings to other individual segmental positions are listed in Tables I and II, which have been made by comparison with previous results,[8,83] and by making use of the partially relaxed ^{2}H NMR spectra.

Figure 2 shows ^{2}H NMR spectra of DMPC-d_{54}:cholesterol (1/1) obtained at various orientations θ of the bilayer normal with respect to the external magnetic field. As can be seen, increasing the tilt angle leads to a decrease of all the quadrupolar splittings, and near the magic angle of $\theta = 54.7°$ the splittings reverse their sign. The inversion recovery pulse sequence followed by the quadrupolar echo[45] was used to measure the spin-lattice relaxation rates (R_{1Z}) at different sample tilt angles θ. Partially relaxed ^{2}H NMR spectra for macroscopically oriented DMPC-d_{54}:cholesterol at $\theta = 90°$ and 76.8 MHz are shown in part (a) of Fig. 3. The broadband Jeener-Broekaert sequence[8,86,87] was used to measure the quadrupolar order relaxation rates (R_{1Q}), from the decay of spectra such as illustrated in part (b) of Fig. 3. By performing these experiments at various sample orientations and NMR frequencies, the angular anisotropies of the ^{2}H R_{1Z} and R_{1Q} relaxation rates were measured. The experimental R_{1Z} and R_{1Q} relaxation rates for the observable resonances measured at 46.1 and 76.8 MHz as a function of sample orientation are summarized in Tables I and II, respectively.

Profiles of the various ^{2}H NMR observables as a function of the acyl segment position (i) are shown in Fig. 4, in which previous results[59] for DMPC-d_{54} are compared to mixed bilayers of DMPC-d_{54}:cholesterol (1/1) (this work) for $\theta = 90°$. The left hand panels depict profiles for $\lvert S_{CD}^{(i)}\rvert$,

TABLE II. Deuterium spin-lattice (R_{1Z}) and quadrupolar order (R_{1Q}) relaxation rates for sn-1 and sn-2 acyl chains of DMPC-d_{54}:cholesterol (1/1) in the liquid-ordered phase at 40 °C and 76.8 MHz.

Reso-	Acyl chain segment[a]			$R_{1Z}(\theta)/s^{-1}$							$R_{1Q}(\theta)/s^{-1}$						
nance	sn-1	sn-2	$\lvert S_{CD}\rvert$	$\theta=0°$	19°	27°	40°	63°	74°	90°	0°	19°	27°	40°	63°	74°	90°
A	2–6	3–6	0.4211	32.8	30.1	25.6	23.6	16.4	14.8	13.9	7.2	8.2	8.8	12.8	15.2	16.5	17.2
				±3.4	±2.0	±2.5	±2.3	±1.3	±1.1	±0.3	±0.8	±0.5	±0.9	±1.1	±1.3	±1.0	±0.8
B	7–8	7–8	0.3875	27.1	24.2	22.1	21.3	15.6	14.1	13.0	9.1	8.4	8.4	13.2	16.0	14.8	14.3
				±2.2	±1.5	±1.8	±1.6	±1.1	±1.0	±0.4	±1.8	±0.6	±0.4	±1.3	±0.9	±1.2	±0.9
C	9,10	9,10	0.3587	23.6	21.3	21.6	20.5	16.5	15.1	13.0	10.1	9.6	10.4	13.3	13.7	13.8	12.5
				±1.5	±2.6	±1.8	±1.8	±1.4	±1.7	±0.3	±1.9	±0.6	±0.6	±0.6	±2.1	±0.9	±0.9
D	11	⋯	0.3207	13.6	14.3	15.0	16.2	13.6	12.5	11.2	10.0	9.5	12.6	11.1	12.2	10.9	7.8
				±0.9	±0.5	±1.1	±1.4	±1.3	±0.9	±0.3	±0.6	±1.2	±0.4	±0.6	±0.7	±0.8	±0.3
E	⋯	12	0.3122	11.3	11.1	12.2	12.7	12.2	9.9	8.4	5.0	7.2	8.5	10.4	10.0	8.7	5.1
				±0.6	±0.2	±0.7	±1.2	±0.5	±0.9	±0.6	±0.5	±1.1	±0.6	±0.8	±1.0	±0.4	±0.2
F	12	⋯	0.2657	8.1	8.5	9.0	9.7	9.8	8.9	8.4	5.9	7.1	8.7	8.0	7.3	6.9	5.4
				±0.2	±0.4	±0.5	±3.4	±0.4	±0.8	±0.6	±0.7	±0.9	±0.3	±0.8	±0.6	±0.4	±0.2
G	⋯	13,2a	0.2401	10.6	10.9	9.5	9.8	9.7	10.7	9.1	4.9	9.9	8.1	8.1	7.6	6.9	6.2
				±0.7	±0.8	±0.6	±0.6	±0.6	±0.8	±0.7	±0.2	±0.6	±0.6	±0.5	±0.4	±0.5	±0.1
H	13	⋯	0.1942	7.0	6.7	6.3	7.2	7.4	7.3	7.0	7.3	6.5	6.1	6.5	5.5	4.8	4.2
				±0.3	±0.5	±0.2	±0.3	±0.1	±0.4	±0.1	±0.4	±0.3	±0.3	±0.4	±0.8	±0.3	±0.3
I	14	⋯	0.0608	2.4	2.5	2.5	2.8	3.4	3.4	3.6	3.1	3.2	2.9	2.6	1.8	2.0	1.9
				±0.3	±0.2	±0.2	±0.4	±0.4	±0.4	±0.5	±0.1	±0.1	±0.4	±0.1	±0.3	±0.2	±0.1

[a]Spectral assignments are from Ref. 84.

$R_{1Z}^{(i)}$, and $R_{1Q}^{(i)}$ for pure DMPC-d_{54} bilayers at 40 °C and 76.8 MHz, whereas the right hand panels show the corresponding data for DMPC-d_{54}:cholesterol (1/1). As discussed previously,[8,59,65] a plateau is observed in both the order parameters $|S_{CD}^{(i)}|$ and the relaxation rates $R_{1Z}^{(i)}$ and $R_{1Q}^{(i)}$ as a function of acyl chain position for DMPC-d_{54}, parts (a), (c), and (e). The major influences of cholesterol, as shown in parts (b), (d), and (f), involve an increase in the order parameters, together with a decrease in the relaxation rates $R_{1Z}^{(i)}$ and $R_{1Q}^{(i)}$ at $\theta=90°$. These results show that the ordering and relaxation rates must both be considered in discussing the properties of lipid bilayers, including correlations of the various quantities.[47]

The possibility of correlation of the order parameters $|S_{CD}^{(i)}|$ and the relaxation rates $R_{1Z}^{(i)}$ and $R_{1Q}^{(i)}$ is considered in Fig. 5 in terms of a square-law functional dependence.[47,90] Figure 5 shows plots of the ^{2}H $R_{1Z}^{(i)}$ and $R_{1Q}^{(i)}$ relaxation rates as a function of the order parameters $|S_{CD}^{(i)}|$ squared for pure DMPC-d_{54} versus DMPC-d_{54}:cholesterol (1/1) at two sample orientations of $\theta=0$ and 90° and frequencies of 46.1 and 76.8 MHz. As can be seen, a nearly linear dependence is observed for pure DMPC-d_{54} bilayers,[59] whereas such a linear dependence is not clearly evident in the case of DMPC-d_{54} bilayers containing cholesterol. It has been argued[47,52,65,90] that the linear dependence may be the result of axially symmetric fast local motions, which preaverage the residual coupling tensor and simply scale the relaxation rates for the whole acyl chain by the corresponding order parameter squared. Note that the ^{2}H R_{1Z} and R_{1Q} relaxation rates for DMPC-d_{54}:cholesterol are in the same general range as for pure DMPC-d_{54}, whereas the substantially smaller acyl chain order parameters in the latter case yield a much steeper slope of the square-law dependence for the ^{2}H

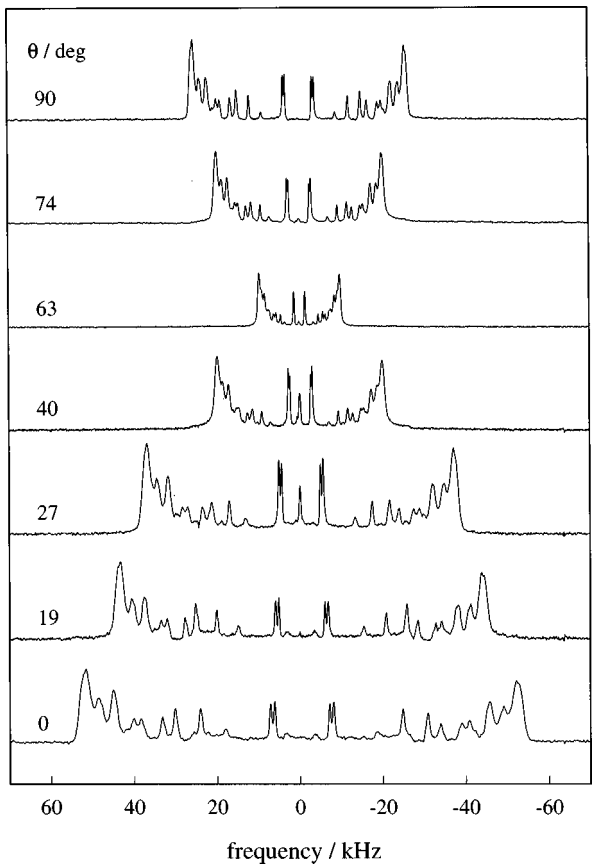

FIG. 2. Experimental ^{2}H NMR spectra acquired at 46.1 MHz for macroscopically oriented DMPC-d_{54}:cholesterol (1/1) bilayers in the liquid-ordered phase at $T=40$ °C as a function of sample tilt angle θ ($\equiv\beta_{DL}$). As the sample tilt is increased from $\theta=0°$, a contraction of the spectrum occurs, such that at the magic angle (54.7°) the quadrupolar splittings reverse sign. Note that at the $\theta=90°$ inclination the splittings are scaled by a factor of $-1/2$ with respect to the $\theta=0°$ tilt spectrum.

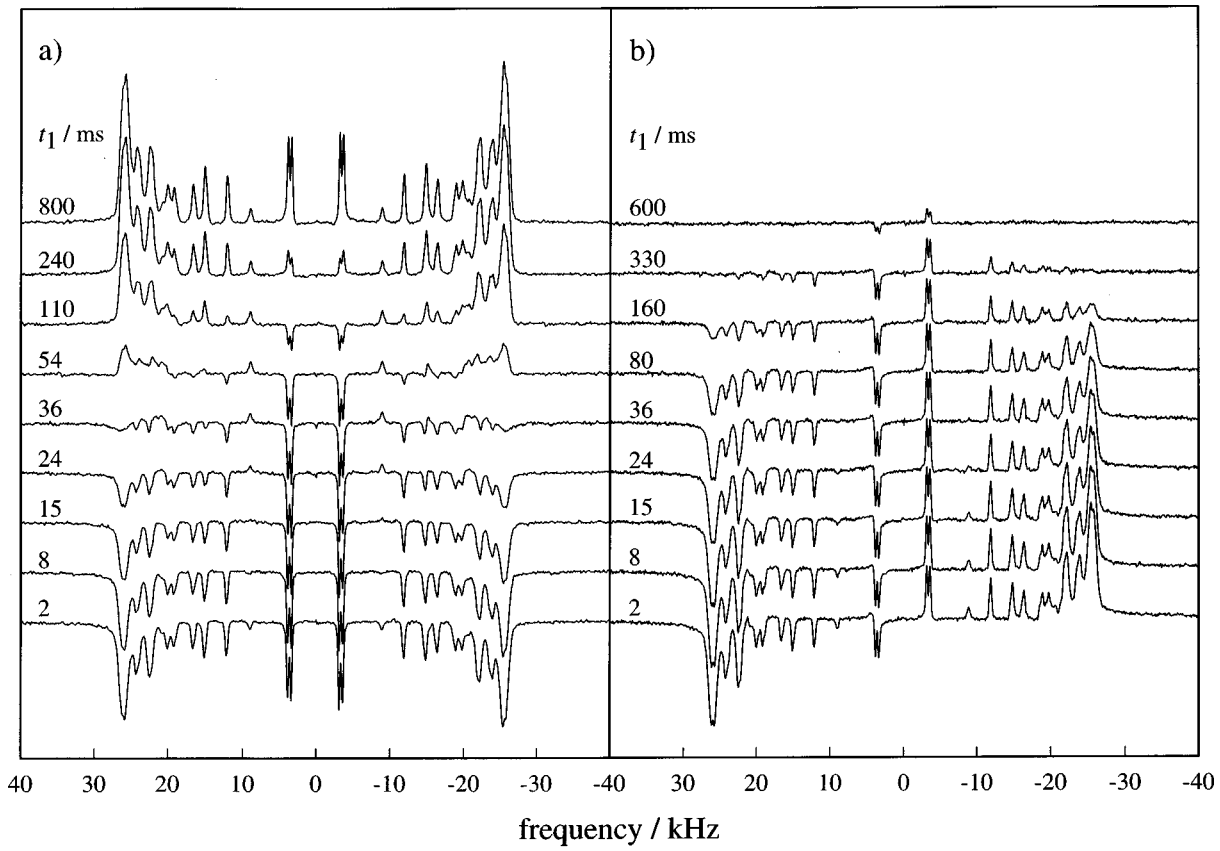

FIG. 3. Partially relaxed ^{2}H NMR spectra at 76.8 MHz for bilayers of DMPC-d_{54}:cholesterol (1/1) macroscopically oriented at $\theta=90°$ in the liquid-ordered phase at $T=40\,°$C. (a) Recovery of Zeeman order (R_{1Z}); and (b) decay of quadrupolar order (R_{1Q}). The inversion recovery pulse sequence followed by the quadrupolar echo (Refs. 45 and 101) was utilized for the ^{2}H R_{1Z} measurements, whereas the broadband Jeener-Broekaert sequence (Refs. 8 and 86) was used for the ^{2}H R_{1Q} measurements. In parts (a) and (b) the partially relaxed ^{2}H NMR spectra are plotted at different delay times (t_1).

R_{1Z} and R_{1Q} relaxation rates of pure lipid bilayers. The nonlinear dependence which is observed for DMPC-d_{54}:cholesterol may point to an effectively asymmetric residual coupling tensor, and, possibly, a variable average orientation of the PAS of the residual coupling tensor along the lipid chain arising from lipid-cholesterol interactions. Apart from the higher molecular ordering in the case of DMPC-d_{54}:cholesterol, this constitutes a second model-independent observation which distinguishes the ^{2}H NMR relaxation rates of cholesterol-containing lipid bilayers from pure phospholipids.

The angular dependencies of the ^{2}H R_{1Z} and R_{1Q} relaxation rates measured at 46.1 and 76.8 MHz for the various acyl chain segments of DMPC-d_{54}:cholesterol (1/1) at 40 °C are illustrated in Fig. 6. The various panels of Fig. 6 correspond to the observable ^{2}H resonances, designated *A* through *I*, as summarized in Tables I and II. A third important observation regarding the influence of cholesterol is that a strong angular anisotropy takes place for the ^{2}H R_{1Z} relaxation rates at the top part of the acyl chain (splittings *A*–*C*). By contrast, for the segments near the terminal methyl group (splittings *G*–*I*), the relaxation rates do not depend strongly on the sample inclination, which is also observed in the case of pure lipid bilayers, albeit for the entire acyl chain.[59,64,65] The above may mean that the effect of cholesterol on the lipid dynamics is more pronounced for the segments that are closer to the glycerol backbone, since the rigid ring system of cholesterol is shorter than the length of the DMPC-d_{54} acyl chains. To further interpret the data, the composite membrane deformation model has been used to simultaneously fit the ^{2}H R_{1Z} and R_{1Q} relaxation rates for the entire acyl chain, as also shown in Fig. 6. An odd potential of mean torque,[49] i.e., $U(\beta_{MN})=-\lambda_1 P_1(\cos\beta_{MN})$, has been used, although the choice of an even potential[47] yields almost identical results (not shown). The parameters of the residual coupling tensor, namely the effective asymmetry parameter η_Q^{eff}, and the orientation of the *z*-axis of the PAS of the residual coupling tensor with respect to the long molecular axis as given by the angle β_{IM}, have been varied along the acyl chain. By using Eq. (3.4), the fast order parameters $S_f^{(2)}$ have been expressed in terms of the observed order parameters S_{CD} and the slow molecular order parameter $S_s^{(2)}$. The other fitting parameters, including the diffusion coefficients $D_\parallel$ and $D_\perp$, the energy parameter λ_j, where $j=1,2$ (or alternatively the slow order parameter $S_s^{(2)}$), as well as the viscoelastic parameter D corresponding to collective motions, have been held the same for all the acyl chain segments. As indicated in Fig. 6, the simultaneous fits of the composite membrane deformation model (solid lines) to the ^{2}H R_{1Z} and R_{1Q} relaxation rates at 46.1 and 76.8 MHz demonstrate the ability of the model to describe the orientational anisotropy of the

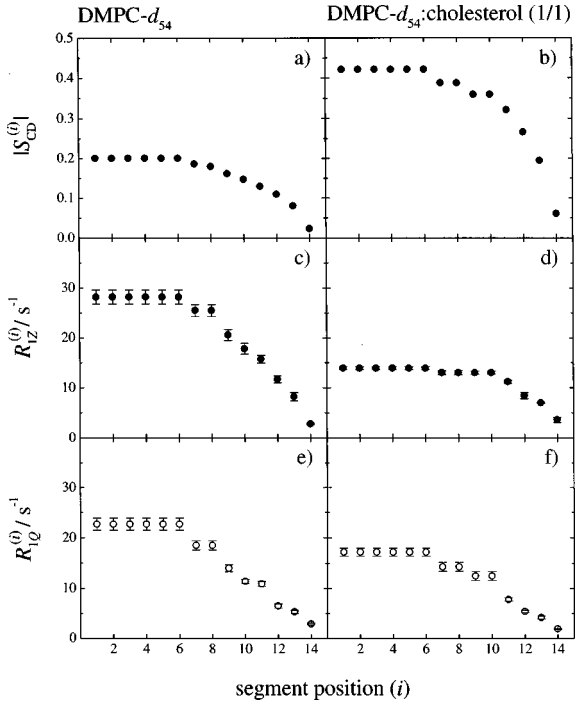

FIG. 4. Comparison of profiles of ^{2}H NMR observables for the sn-1 acyl chain of DMPC-d_{54} in the L_α phase versus mixed bilayers of DMPC-d_{54}:cholesterol (1/1) in the liquid-ordered phase at $T=40\,^\circ$C, with a sample tilt of $\theta=90°$. Parts (a), (c), and (e) depict profiles of the order parameters $|S_{CD}^{(i)}|$ and relaxation rates $R_{1Z}^{(i)}$ and $R_{1Q}^{(i)}$ plotted as a function of the acyl segment position (i) for pure DMPC-d_{54} bilayers at 76.8 MHz. Parts (b), (d), and (f) show the corresponding data for DMPC-d_{54}:cholesterol (1/1) bilayers. A plateau is observed for both the order parameters $|S_{CD}^{(i)}|$ and the $R_{1Z}^{(i)}$ and $R_{1Q}^{(i)}$ relaxation rates. The major influences of cholesterol involve an increase in the values of the order parameters, together with a decrease in the relaxation rates $R_{1Z}^{(i)}$ and $R_{1Q}^{(i)}$ at $\theta=90°$.

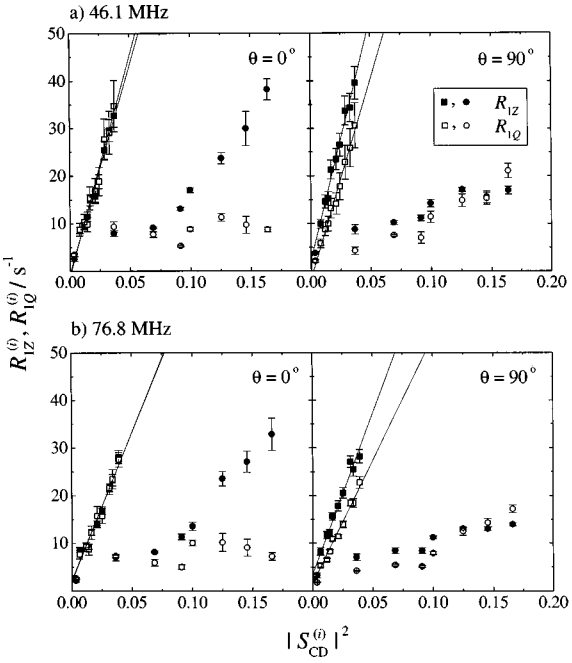

FIG. 5. Experimental ^{2}H NMR $R_{1Z}^{(i)}$ and $R_{1Q}^{(i)}$ relaxation rates of lipid bilayers plotted versus the square of the experimentally observed order parameters $|S_{CD}^{(i)}|$, showing the influence of cholesterol. Data include $R_{1Z}^{(i)}$ (■) and $R_{1Q}^{(i)}$ (□) relaxation rates for bilayers of DMPC-d_{54}, and $R_{1Z}^{(i)}$ (●) and $R_{1Q}^{(i)}$ (○) relaxation rates for DMPC-d_{54}:cholesterol (1/1) in the liquid-ordered phase at $T=40\,^\circ$C: (a) 46.1 MHz; and (b) 76.8 MHz at macroscopic sample tilt angles of $\theta=0$ and 90°. Note that the slope of the dependence of the $R_{1Z}^{(i)}$ and $R_{1Q}^{(i)}$ relaxation rates on the square of the order parameter is much steeper for pure lipid bilayers than for cholesterol containing bilayers, as a result of the lower ordering in the former case. A linear functional dependence is observed for pure DMPC-d_{54} bilayers along the entire acyl chain at the various sample tilt angles, Ref. 59, which is not the case for DMPC-d_{54} bilayers containing cholesterol. The latter may be a consequence of nonaxially symmetric segmental motions, yielding a nonzero effective asymmetry parameter, and possibly a variation of the PAS of the residual coupling tensor along the acyl chain due to the degree of lipid chain entanglement.

nuclear spin relaxation of DMPC-d_{54} bilayers containing cholesterol simultaneously for the entire acyl chain, except for some deviations in the case of splittings $D-F$. This may be due to the fact that the corresponding peaks in the ^{2}H NMR spectrum are highly overlapping, and thus yield slightly inaccurate observable relaxation rates.

One should note that the molecular diffusion model,[47–49,65] i.e., when only noncollective molecular motions are considered, can be recovered as a limiting case from the composite membrane deformation model by setting the parameter D to zero in Eqs. (3.3) and (3.8). The fits to the molecular diffusion model assuming an odd potential of mean torque (dashed lines) in Fig. 6 yield similar results to the composite membrane deformation model, except for a slightly worse quality of the fits to the relaxation data for the plateau region (splitting A). The corresponding fitting parameters are summarized in Table III. As can be seen, even though the results are similar in both cases, inclusion of collective motions yields a dramatic decrease in the diffusion coefficient $D_\perp$ which would mean that off-axial diffusion does not contribute predominantly to the nuclear spin relaxation of lipid bilayers in the mid-MHz range.

Figure 7 shows the parameters of the residual coupling tensor obtained from the fits, which are plotted as a function of the position (i) in the lipid sn-1 acyl chain. Part (a) of Fig. 7 illustrates that the values of the angle $\beta_{IM}^{(i)}$, describing the orientation of the z-axis of the PAS of the residual coupling tensor with respect to the long molecular axis, are similar for both the composite membrane model and the molecular diffusion model. They vary along the chain from 90° for the plateau region to about 65° for the terminal methyl group (or alternatively 115°, since one cannot distinguish between $\beta_{IM}^{(i)}$ and $\pi-\beta_{IM}^{(i)}$ due to the even parity of the quadrupolar interaction). Both the composite membrane deformation model and the molecular diffusion model yield a variable asymmetry parameter $\eta_Q^{\mathrm{eff}(i)}$ having its largest absolute value for the plateau region (splitting A) and zero values for the terminal segments; cf. part (b) of Fig. 7. Using Eq. (3.4), the corresponding fast order parameter $S_f^{(2)}$, and therefore the effective coupling constant $\chi_Q^{\mathrm{eff}(i)}$, can be determined. As can be seen from part (c) of Fig. 7, the values of the effective coupling constant decrease progressively along the acyl chain as a result of an increase in the motional disorder toward the center of the bilayer.

As the next step of the experimental data reduction, the laboratory-frame spectral densities of motion $J_1(\omega_D,\beta_{DL})$ and $J_2(2\omega_D,\beta_{DL})$ have been directly calculated for various

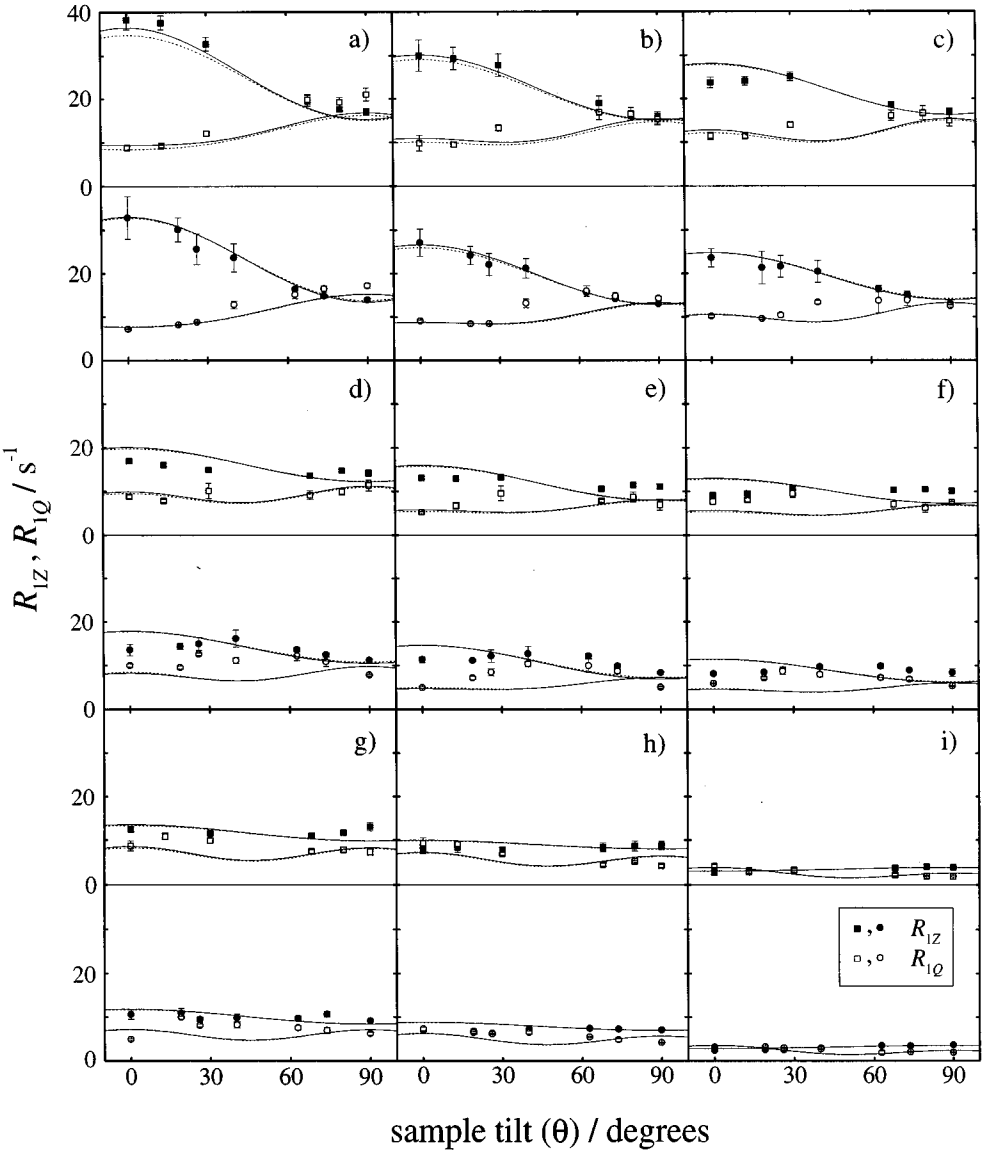

FIG. 6. Experimental ^{2}H R_{1Z} and R_{1Q} relaxation rates as a function of bilayer orientation and simultaneous theoretical fitting to composite membrane deformation model at two different frequencies (magnetic field strengths). Parts (a)–(i) indicate ^{2}H R_{1Z} relaxation rates at 46.1 (■) and 76.8 MHz (●), and R_{1Q} relaxation rates at 46.1 (□) and 76.8 MHz (○) for the resolved quadrupolar splittings (designated $A-I$) of DMPC-d_{54}:cholesterol (1/1) as a function of bilayer orientation, in the liquid-ordered phase at $T=40\,^{\circ}$C. Assignments of the ^{2}H NMR splittings to individual acyl chain segments are given in Tables I and II. Results are shown for the composite membrane deformation model including both molecular and collective motions (——), as well as for the limiting case of molecular motions only (----). The data are summarized in Tables I and II and the fitting parameters are presented in Table III. In both cases an adequate fit is obtained, suggesting that collective motions do not appreciably affect the nuclear spin relaxation in lipid bilayers containing cholesterol. The discrepancy between theory and experiment for resonances $D-F$ may be due to the fact that the corresponding peaks are not well resolved in the ^{2}H NMR spectra.

positions in the lipid acyl chain by using Eqs. (2.1) and (2.2). Figure 8 reveals that for segments close to the lipid head group (splittings $A-C$), the spectral densities follow the trend $J_1(\omega_D,\beta_{DL})<J_2(2\omega_D,\beta_{DL})$ when the tilt angles β_{DL} are less than approximately the magic angle (54.7°), and $J_1(\omega_D,\beta_{DL})>J_2(2\omega_D,\beta_{DL})$ otherwise. This tendency appears to be reversed for the segments close to the end of the acyl chain (splittings $G-I$). As also shown in Fig. 8, the above trends can be described in general by the theoretical spectral densities calculated using the composite membrane deformation model, with the parameters obtained from the fitting to the ^{2}H R_{1Z} and R_{1Q} relaxation rates; cf. Table III. However, for splittings $D-F$ the model predicts the same behavior as for resonances $A-C$, which is less evident from the experimental data. In addition, for splittings $G-I$ the model predicts two crossing points of the spectral densities $J_1(\omega_D,\beta_{DL})$ and $J_2(2\omega_D,\beta_{DL})$. The above discrepancies with experimental data may be due to the fact that the corresponding peaks are not clearly resolved in the ^{2}H NMR spectra of DMPC-d_{54}:cholesterol; cf. part (a) of Fig. 1.

Finally, for the composite membrane deformation model, the relative contributions to the ^{2}H R_{1Z} relaxation rates from molecular diffusion, collective motions, and the cross term, cf. Eq. (3.9), have been calculated for the plateau region (splitting A; acyl chain segments C2–C6). The results for DMPC-d_{54}:cholesterol (1/1) are plotted as a function of

TABLE III. Summary of parameters for fits to ^{2}H spin-lattice (R_{1Z}) and quadrupolar order (R_{1Q}) relaxation rates of DMPC-d_{54}:cholesterol (1/1) in the liquid-ordered phase at 40 °C.[a]

Resonance	Motions	Parameter								
		$D_\parallel/10^9\ s^{-1}$	$D_\perp/10^6\ s^{-1}$	λ_1/kT	$S_s^{(2)}$	$D/10^{-7}\ s^{1/2}$	α_{IM}/deg	β_{IM}/deg[c]	η_Q^{eff}	χ_Q^{eff}/kHz
A	Molecular + collective	5.43 ±0.32	0.399 ±0.249	40.0[b]	0.927	4.91 ±0.45	90	90[d]	0.1[b]	171.6 ±9.3
	Molecular only	5.52 ±0.33	62.0 ±4.4	40.0[b]	0.927	0	90	90[d]	0.1[b]	171.6 ±9.3
B	〃	〃	〃	〃	〃	〃	〃	84.4 ±0.4	0.062 ±0.011	156.2 ±11.1
	〃	〃	〃	〃	〃	〃	〃	83.6 ±0.8	0.034 ±0.023	153.6 ±11.2
C	〃	〃	〃	〃	〃	〃	〃	81.4 ±0.6	0.034 ±0.027	146.2 ±13.8
	〃	〃	〃	〃	〃	〃	〃	80.7 ±0.8	0.010 ±0.036	148.9 ±13.9
D	〃	〃	〃	〃	〃	〃	〃	81.5 ±0.7	0[d]	125.9 ±8.2
	〃	〃	〃	〃	〃	〃	〃	81.0 ±0.5	0[d]	127.0 ±8.2
E	〃	〃	〃	〃	〃	〃	〃	85.9 ±1.3	0[d]	116.2 ±7.4
	〃	〃	〃	〃	〃	〃	〃	84.4 ±0.7	0[d]	116.5 ±8.0
F	〃	〃	〃	〃	〃	〃	〃	83.1 ±0.9	0[d]	101.9 ±6.8
	〃	〃	〃	〃	〃	〃	〃	82.3 ±0.8	0[d]	98.2 ±8.4
G	〃	〃	〃	〃	〃	〃	〃	78.0 ±0.5	0[d]	101.2 ±6.6
	〃	〃	〃	〃	〃	〃	〃	77.6 ±0.4	0[d]	102.3 ±6.8
H	〃	〃	〃	〃	〃	〃	〃	76.1 ±1.0	0[d]	86.2 ±7.2
	〃	〃	〃	〃	〃	〃	〃	76.2 ±1.1	0[d]	87.3 ±6.3
I	〃	〃	〃	〃	〃	〃	〃	65.7 ±0.1	0[d]	45.4 ±2.8
	〃	〃	〃	〃	〃	〃	〃	65.9 ±0.1	0[d]	47.0 ±2.9

[a]All curve fitting has been done by using the Levenberg-Marquardt algorithm. The fits have been statistically weighted by the inverse squares of the standard deviations of the individual data points (Ref. 102). An odd potential of mean torque, $U(\beta_{MN}) = -\lambda_1 P_1(\cos\beta_{MN})$, has been assumed for molecular reorientations.

[b]Parameter was held fixed at the indicated value to satisfy the condition $S_f^{(2)} \lesssim 1$.

[c]Supplementary angles $\pi - \beta_{IM}$ are indistinguishable from β_{IM} due to the even parity of the quadrupolar interaction and are not included.

[d]Parameter was held constant at the indicated value since it cannot be determined to within an applicable accuracy from the fits.

the sample tilt angle (θ) in Fig. 9, part (a). As can be seen, molecular rotational diffusion appears to be the predominant relaxation mechanism, in agreement with earlier conclusions,[8] whereas the contribution from the collective motions is appreciably smaller. Similar results are obtained for other acyl segments (not shown). Part (b) of Fig. 9 shows the contributions from different motions obtained from fitting the frequency and angular dependent ^{2}H R_{1Z} and R_{1Q} relaxation rates for pure DMPC-d_{54}.[59] In this case, the contributions from molecular and collective motions, as well as from the cross term, are found to be comparable. The above may indicate an increased dynamical rigidity of the cholesterol-containing bilayers versus pure lipid bilayers, consistent with micromechanical deformation studies.[34]

VI. DISCUSSION

Nuclear spin relaxation studies of lipid bilayers containing cholesterol in the liquid-ordered phase[20,23] constitute a powerful means for investigating its effects on the dynamical properties of biological membranes. As a rule, the relaxation of lipid bilayers can include contributions from (i) internal (local) motions due to *trans-gauche* isomerizations of the chains; (ii) overall motions of the lipids due to restricted rotational diffusion; and (iii) collective excitations of the lipid bilayer formulated as collective order-director fluctuations (ODF).[47] The different effects of cholesterol on the ordering and ^{2}H NMR relaxation rates of the phospholipids evince clearly that both the molecular ordering and reorientational dynamics need to be considered in relation to their physical properties.[91] We have recently suggested that the combined orientational anisotropy and frequency dependence of the R_{1Z} and R_{1Q} relaxation rates of lipid bilayers in the liquid-crystalline state can be explained in terms of a composite membrane deformation model, which includes the additional influences of axial rotations of the lipids.[59] The

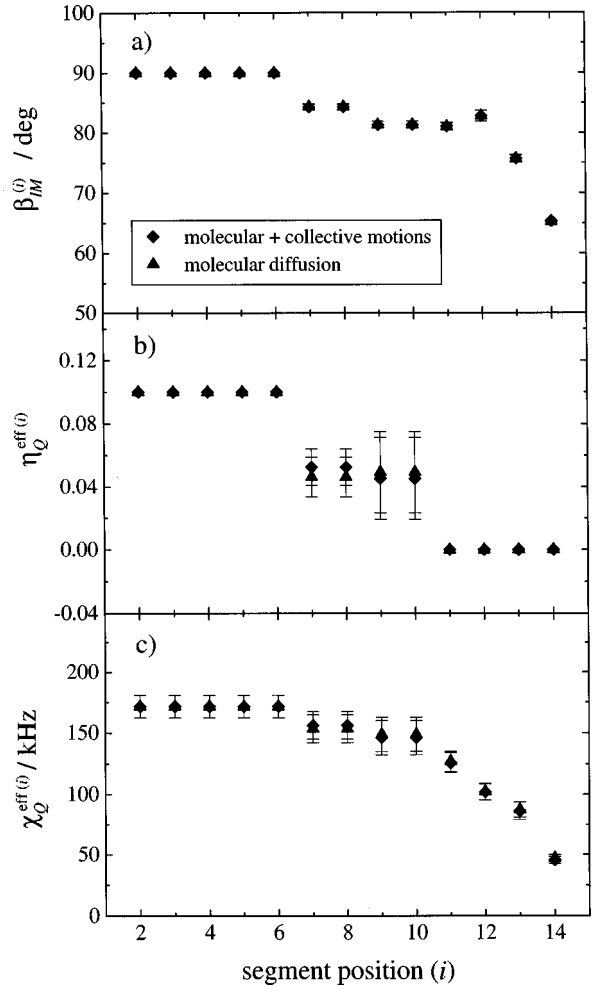

FIG. 7. Parameters of residual coupling tensor versus sn-1 acyl chain position obtained from fitting the composite membrane deformation model to ^{2}H R_{1Z} and R_{1Q} relaxation rates for DMPC-d_{54}:cholesterol (1/1) in the liquid-ordered phase at $T=40\,^\circ$C. Results are presented for the composite model (◆), which includes both molecular and collective motions, and for the case of molecular motions only (▲). (a) Profiles of the angle $\beta_{IM}^{(i)}$ describing the orientation of the z-axis of the PAS of the residual coupling tensor. The values decrease along the chain from 90 to 65°; supplementary angles $\pi-\beta_{IM}^{(i)}$ are indistinguishable from $\beta_{IM}^{(i)}$ due to the even parity of the quadrupolar interaction. (b) Behavior of the effective asymmetry parameter $\eta_Q^{\mathrm{eff}(i)}$. The composite membrane deformation model predicts the highest values of $\eta_Q^{\mathrm{eff}(i)}\approx 0.1$ for splitting A (plateau region), decreasing to zero for splittings $D-I$, which implies that effective fast motions of acyl segments close to the terminal group are axially symmetric even if cholesterol is present. (c) Profiles of the effective coupling constant $\chi_Q^{\mathrm{eff}(i)}$, which decreases along the acyl chain as a result of lower segmental ordering.

composite deformation model represents a new framework for analyzing the dynamics of membrane lipids in the liquid-crystalline state.

Here the orientational anisotropies of the ^{2}H R_{1Z} and R_{1Q} relaxation rates of DMPC-d_{54}:cholesterol (1/1 molar ratio) have been measured at frequencies of 46.1 and 76.8 MHz and a temperature of 40 °C. Data for the entire acyl chain have been analyzed using the above-mentioned composite membrane deformation model.[59] The model considers the influences of fast segmental reorientations in terms of preaveraged motional amplitudes due to fast (on the ^{2}H NMR scale) chain motions, which yield a residual coupling tensor having an effectively nonzero asymmetry parameter. Combined influences of slower three-dimensional collective fluctuations, together with effective axial rotations of the lipid molecules, are assumed to modulate the residual coupling tensor due to the local motions, and predominantly govern the orientational anisotropy and frequency dependence of the relaxation. The composite membrane deformation model yields expressions for the spectral densities in closed form, and fits the anisotropic relaxation data for the DMPC-d_{54}:cholesterol (1/1) bilayers simultaneously at the two different frequencies, 46.1 and 76.8 MHz, for all the observable acyl resonances. For the case of the cholesterol-containing DMPC-d_{54} bilayers, a relatively high asymmetry parameter for the residual coupling tensor of $\eta_Q^{\mathrm{eff}}\approx 0.1$ is needed to account for the strong angular anisotropy of the segments close to the lipid head group (plateau region) at both frequencies, whereas for pure phospholipid bilayers the data can be fit with a zero effective asymmetry parameter for the whole acyl chain.[59,65] The above may be the result of interactions between the lipid chains and the rigid cholesterol ring system, which decrease the number of rotameric degrees of freedom for the upper part of the acyl groups, thus yielding nonaxially symmetric effective local motions associated with a nonzero asymmetry parameter. Moreover, in the case of DMPC-d_{54}:cholesterol, the orientation of the z-axis of the PAS of the residual coupling tensor is found to vary along the acyl chain, ranging from a value of $\beta_{IM}=90°$ for the plateau region to $\beta_{IM}=65°$ for the terminal methyl group.

By contrast, the relaxation rates for pure lipid bilayers appear to be scaled by the corresponding order parameter S_{CD} squared for the entire acyl chain.[47,59,65,90] This observation suggests a constant orientation of the residual PAS for all segments, and an axially symmetric nature of the effective local segmental reorientations. The different results for the mixed bilayers containing cholesterol can be interpreted simply as an effect of increased chain entanglement near the center of the bilayer, e.g., due to different lengths of the rigid cholesterol ring system and flexible lipid molecules. The favorable interactions between the cholesterol and phosphatidylcholine molecules change the asymmetry parameter and the orientation of the PAS of the residual coupling tensor along the lipid acyl chains. Hence, the top part of the chain remains highly ordered by the rigid cholesterol molecule,[15,20,92] whereas the chain segments deeper in the bilayer are in contact with the flexible cholesterol tail and are more entangled as in the case of pure lipid bilayers. Interestingly, if only noncollective molecular motions are considered,[8] the overall quality of the fits to the ^{2}H R_{1Z} and R_{1Q} relaxation rates of DMPC-d_{54}:cholesterol (1/1) does not change appreciably. This suggests a rather small contribution from collective motions to the nuclear spin relaxation in cholesterol-containing bilayers as a result of an increased dynamical rigidity versus pure lipid bilayers.

It is interesting to compare the present results with earlier spin label EPR studies[17,21,37,91] and also previous NMR studies of cholesterol:phospholipid interactions.[4,8,9] Both EPR results for the cholestane spin label[21] and the present membrane deformation model yield relatively small values for the off-axial diffusion coefficient ($D_\perp$ on the order of

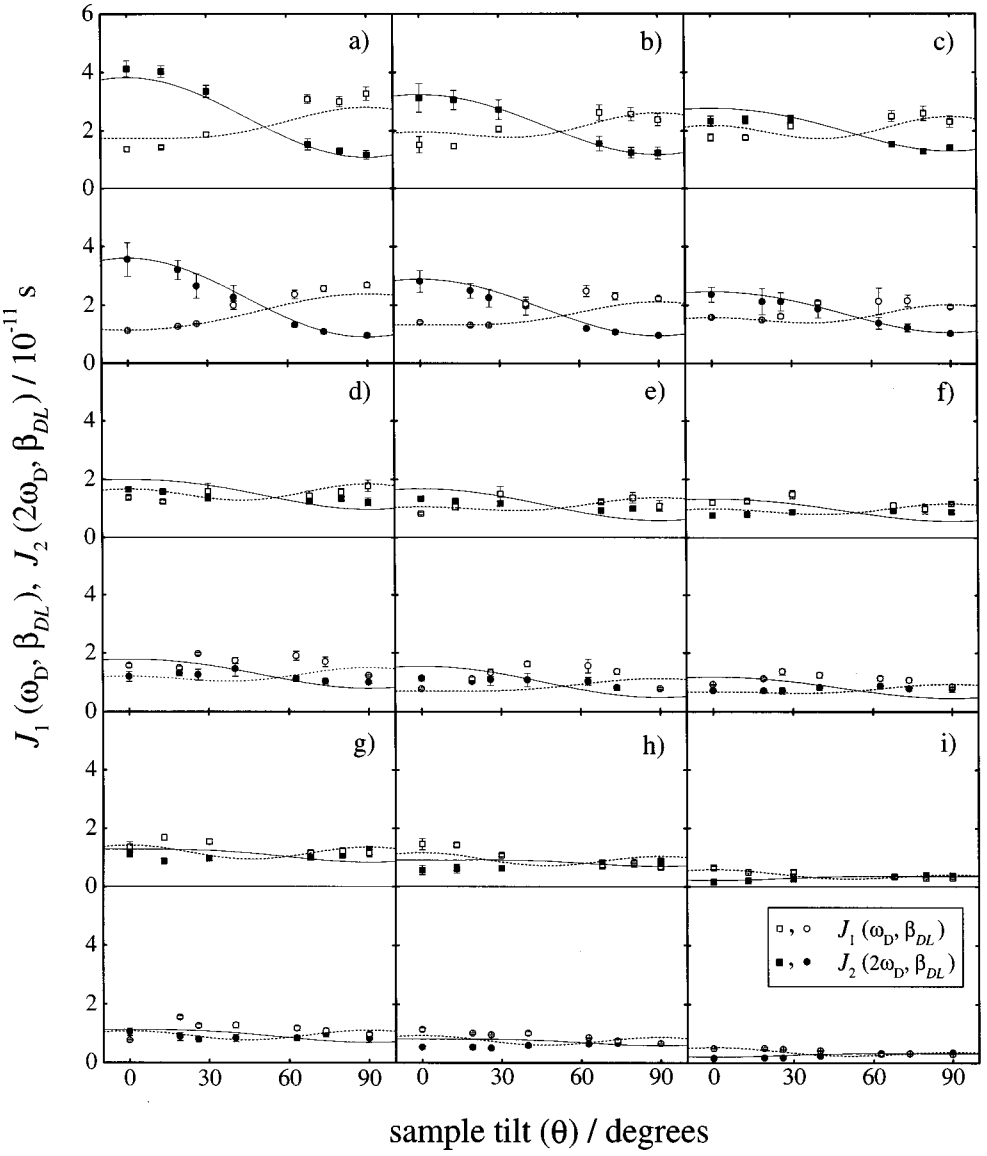

FIG. 8. Laboratory-frame spectral densities of motion calculated from experimental ^{2}H R_{1Z} and R_{1Q} relaxation rates at two different frequencies (magnetic field strengths) as a function of bilayer orientation. Parts (a)–(i) indicate spectral densities $J_1(\omega_D,\beta_{DL})$ at 46.1 (□) and 76.8 MHz (○), and $J_2(2\omega_D,\beta_{DL})$ at 46.1 (■) and 76.8 MHz (●) for resolved quadrupolar splittings (designated $A-I$), of DMPC-d_{54}:cholesterol (1/1), in the liquid-ordered phase at $T=40$ °C. Assignments of the ^{2}H NMR splittings to individual acyl chain segments are given in Tables I and II. The segments closer to the lipid head group (splittings $A-C$) show the trend $J_1(\omega_D,\beta_{DL})<J_2(2\omega_D,\beta_{DL})$ when $\beta_{DL}\lesssim 54.7°$ and $J_1(\omega_D,\beta_{DL})>J_2(2\omega_D,\beta_{DL})$ when $\beta_{DL}\gtrsim 54.7°$; for other segments (splittings $G-I$) this tendency appears to be reversed. The composite membrane deformation model with the fitting parameters summarized in Table III predicts an analogous trend for the theoretical spectral densities $J_1(\omega_D,\beta_{DL})$ (----) and $J_2(2\omega_D,\beta_{DL})$ (——). However, the model predicts the same behavior for splittings $A-C$ as for resonances $D-F$, and for splittings $G-I$ the model predicts two crossing points of the spectral densities. The differences versus the experimental data may represent the fact that the corresponding peaks are not fully resolved in the ^{2}H NMR spectra of DMPC-d_{54}:cholesterol bilayers.

$10^5-10^6\,s^{-1}$), as well as a high molecular ordering of $S_s^{(2)}>0.9$ in the presence of a large mole fraction of cholesterol in the bilayer. However, the present ^{2}H NMR relaxation analysis yields greater values for the axial diffusion coefficient ($D_\parallel=5.43\times10^9\,s^{-1}$) of the phospholipid molecules than those obtained[21] for the cholestane spin probe ($D_\parallel\approx10^8\,s^{-1}$). An earlier ^{2}H NMR investigation of the influences of cholesterol on the dynamics of phospholipid bilayers has been also carried out by Weisz *et al.*,[9] which is complementary to the present study. These authors have analyzed in detail ^{2}H NMR relaxation rates of DMPC and cholesterol in mixed bilayers, having specifically deuterated positions, by measuring the orientation and temperature dependence of the relaxation at a single frequency (magnetic field strength) (46.1 MHz). By contrast, in the present work the entire acyl chain of DMPC-d_{54} has been studied, including the orientational anisotropy of R_{1Z} and R_{1Q} at two frequencies (magnetic field strengths). The approach of Weisz *et al.*[9] is based on numerical solution of the Liouville-von Neumann equation to describe the ^{2}H NMR relaxation rates of DMPC:cholesterol bilayers at 46.1 MHz containing 40 mole % cholesterol. A composite motional process has also been considered by treating fast segmental reorientations as jumps on a diamond lattice, and the molecular reorientations

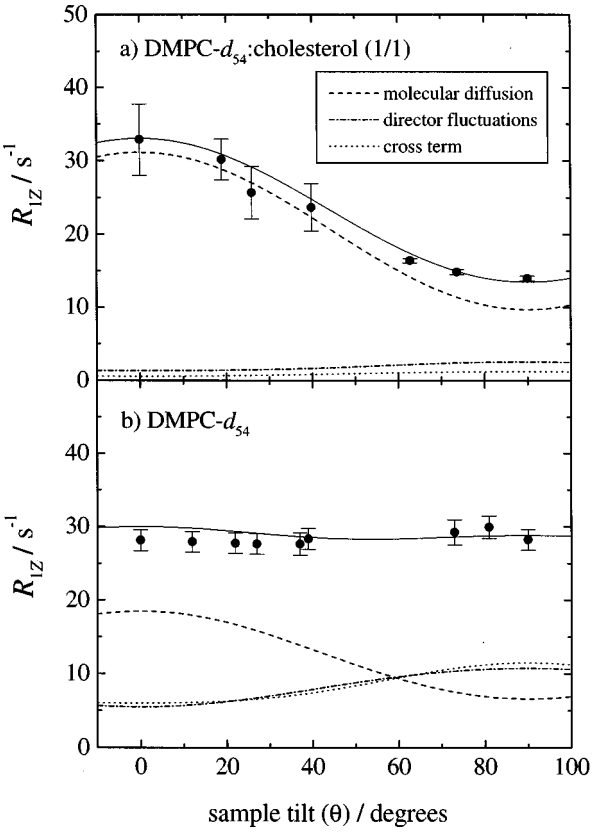

FIG. 9. Contributions from molecular motions, collective fluctuations, and the cross term to the ^{2}H R_{1Z} relaxation rates of oriented bilayers, showing the effect of cholesterol as given by the composite membrane deformation model. (a) DMPC-d_{54}:cholesterol (1/1); and (b) DMPC-d_{54}. Representative data at 76.8 MHz and $T=40\,^{\circ}$C correspond to splitting A (plateau region), comprising acyl chain segments C2-C6. Theoretical R_{1Z} values (——), molecular diffusion contribution (----), director fluctuation contribution (-·-·-), and the cross term (····) are shown. Note that molecular diffusion is predominant for the nuclear spin relaxation in the case of cholesterol-containing DMPC-d_{54} bilayers. However, for pure DMPC-d_{54}, the contributions from molecular and collective motions are comparable, part (b), which may indicate an increased dynamical rigidity of bilayers containing cholesterol versus pure lipid bilayers.

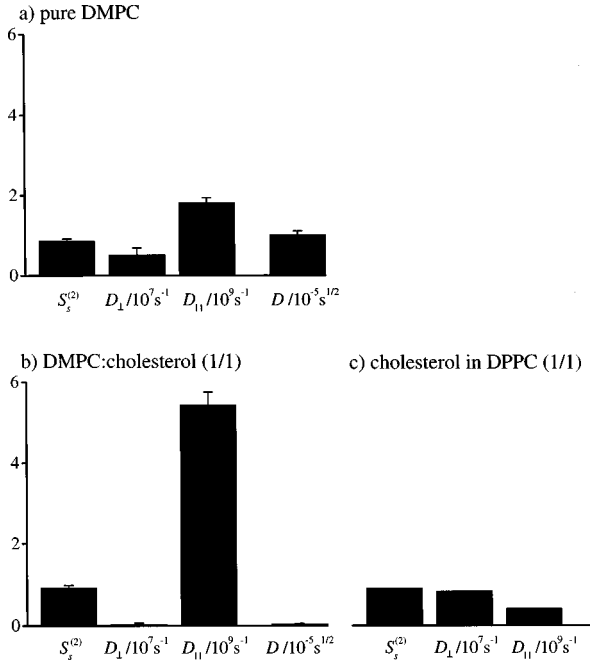

FIG. 10. Summary of dynamical parameters for pure lipid bilayers versus mixed systems obtained from ^{2}H NMR relaxation. (a) DMPC-d_{54} in the liquid-crystalline (L_α) phase at 40 °C; (b) DMPC-d_{54} component of mixture with cholesterol (1/1) in the liquid-ordered phase at 40 °C; and (c) cholesterol component of mixture with DPPC (1/1) in the liquid-ordered phase at 30 °C. For pure lipid bilayers, part (a), the viscoelastic parameter D corresponding to collective motions is appreciably larger than in cholesterol-containing bilayers, part (b), which indicates an increased rigidity in the latter case. Moreover, parts (a) and (b) suggest that a reduction in the off-axial diffusion coefficient $D_\perp$ due to cholesterol is accompanied by an increase in the axial diffusion coefficient $D_\parallel$. Such behavior evinces a reduction in the degree of chain entanglement of the flexible lipid molecules in the presence of cholesterol, leading to a dimunition of the friction coefficient. On the other hand, the axial diffusion coefficient for the cholesterol molecule itself, part (c), is found to be less than the corresponding values for the phospholipids. This is perhaps expected due to the larger effective radius of cholesterol compared to the phospholipid acyl segments, together with the noncylindrical shape and the lack of significant internal degrees of freedom of the rigid sterol ring system.

as anisotropic diffusion having two correlation times, due to the axial rotation around the long molecular axis ($\tau_{R\parallel}$) and the rocking motion of the lipid molecule ($\tau_{R\perp}$). Collective deformations have been treated as two-dimensional director fluctuations[50,93] rather than three-dimensional excitations;[47,59] these are assumed to primarily contribute to the relaxation at lower frequencies, below the MHz regime of the R_{1Z} and R_{1Q} measurements. From such an analysis, it has been concluded that cholesterol significantly reduces the spectral density of the collective motions compared to pure lipid bilayers, which is in agreement with earlier work by Trouard *et al.*[8]

The composite membrane deformation model allows one to calculate directly the contributions from various motions to the observable relaxation rates, and similarly predicts a smaller influence of collective motions formulated as three-dimensional director fluctuations in the case of lipid bilayers containing cholesterol. As noted above, this is in agreement with an earlier preliminary report.[8] A summary of the dynamical parameters for pure lipid bilayers versus mixed systems, obtained from the analysis of ^{2}H NMR relaxation data, is depicted in Fig. 10. Comparison of the viscoelastic parameter D, corresponding to collective motions, with that previously reported for pure DMPC-d_{54} bilayers[59] indicates a decrease of over an order of magnitude in the case of DMPC-d_{54}:cholesterol (1/1), i.e., 68.1×10^{-7} s$^{1/2}$ versus 4.91×10^{-7} s$^{1/2}$. Within the present framework, this results in a decreased slope of the plots of the ^{2}H R_{1Z} and R_{1Q} relaxation rates as a function of the order parameter S_{CD} squared. Taking into account that for three-dimensional director fluctuations[47,77] $D\propto K^{-3/2}\eta^{1/2}$, and assuming the bilayer viscosity η does not change appreciably with the inclusion of cholesterol, one concludes that a nearly sixfold increase in the bilayer elastic constant K occurs in the latter case. On the other hand, Weisz *et al.*[9] report a factor of 3.5 by treating the collective motions as two-dimensional director fluctuations.[50]

It is also of interest to consider the rotational diffusion coefficients of the phospholipid and cholesterol molecules in the mixed bilayers in terms of coupling of their dynamics. Qualitatively, the results of the composite membrane defor-

mation model are generally consistent with previous ^{13}C NMR studies of the carbonyl carbons of DMPC in bilayers containing cholesterol.[94] The observed change of the chemical shift anisotropy of the *sn*-1 carbonyl resonance in DMPC due to the inclusion of cholesterol has been shown to increase the molecular order, with a persistence of fast axial diffusion about the long axis of the molecule.[94] Recall that the composite membrane deformation model[59] describes the dynamics in terms of three-dimensional excitations with wavelengths on the order of the bilayer thickness or less, together with effective axial rotations of the phospholipids. The axial motions are described by the rotational diffusion constant $D_{\|}$, with the off-axis motions corresponding to ODF, plus any additional minor influences which are modeled in terms of the off-axial diffusion constant $D_{\perp}$. It is interesting that according to the composite model, the axial diffusion coefficient $D_{\|}$ corresponding to the rotation about the long axis of the phospholipids appears greater for the DMPC-d_{54}:cholesterol (1/1) bilayers ($D_{\|}=5.43\times10^{9}\,s^{-1}$) than for pure DMPC-$d_{54}$ bilayers ($D_{\|}=1.82\times10^{9}\,s^{-1}$);[59] cf. Fig. 10. On the other hand, the composite membrane deformation model predicts relatively small values for the perpendicular diffusion coefficient, with a decrease for the DMPC-d_{54}:cholesterol (1/1) bilayers ($D_{\perp}=0.399\times10^{6}\,s^{-1}$) versus pure DMPC-$d_{54}$ ($D_{\perp}=5.23\times10^{6}\,s^{-1}$).[59] The former case corresponds to the correlation time $\tau_{R\perp}$ occurring on the microsecond time scale in agreement with the results of Weisz *et al.*[9] As remarked previously, this may be correlated with the effect of cholesterol on the off-axial collective excitations modeled as ODF. However, if only molecular motions are considered as a limiting case, values of the off-axial rotational diffusion constant of about two orders of magnitude greater are found ($D_{\perp}=62.0\times10^{6}\,s^{-1}$). It follows that when treating transverse displacements it may be more consistent to consider only the collective ODF contribution, and neglect specific consideration of the noncollective off-axial rotations.

Physically, the values obtained for the various relaxation parameters using the composite model would lead to the following simple picture for the mobility of the phospholipid molecules in the mixed bilayer. The composite model suggests the lipid relaxation in the MHz range is mainly governed by the superimposed effects of collective order-director fluctuations plus effective axial diffusion of the lipids.[59] According to this framework,[59] in the presence of cholesterol the order-director fluctuations of the lipids are essentially damped out in the MHz regime, so that the remaining dominant contribution to the relaxation arises from phospholipid axial diffusion. We find, moreover, that the axial diffusion of the phospholipids in the presence of cholesterol may be somewhat *faster* than in the pure lipid bilayer. This can perhaps be explained by a reduction in the degree of chain entanglement of the flexible lipid molecules in the presence of cholesterol,[2] e.g., due to a reduction of the friction coefficient. This would lead to an increase in the rate of axial diffusion, since the molecule or the acyl chain is able to rotate more freely.[8]

In addition, one can contrast the nuclear spin relaxation of the phospholipid molecules (this work) with the relaxation of the cholesterol molecule itself in lipid bilayers.[67,68] The presence of a fused ring system means that cholesterol is a very rigid molecule, so that the lack of appreciable segmental motions simplifies its internal dynamics compared to the acyl chains of phospholipids.[67,68,95,96] This allows one to set $S_f^{(2)}=1$ for cholesterol in the composite membrane deformation model, or, alternatively, the molecular diffusion model. The angular dependence of R_{1Z} for specifically labeled cholesterol in a similar bilayer system, 1,2-dipalmitoyl-*sn*-glycero-3-phosphocholine (DPPC)[68] at 30 °C has been explained using an anisotropic rotational diffusion model for molecular reorientations,[96] which is a limiting case of the more general composite membrane deformation model.[59] The model assumes a static EFG tensor unaltered by internal motions ($\chi_Q=170$ kHz, $\eta_Q=0$). It was assumed that both the lipid and cholesterol molecules exhibit high ordering,[5,6,24,25,67,68,89] with molecular order parameters $S_s^{(2)}$ of about 0.9. Application of the composite membrane deformation model suggests that the phospholipid mobility as characterized by $D_{\|}$ may be somewhat greater than in the case of the cholesterol molecule. As can be seen from Fig. 10, for the phospholipid molecules the axial diffusion coefficient ($D_{\|}=54.3\times10^{8}\,s^{-1}$) obtained from the analysis of the ^2H R_{1Z} rates is about tenfold larger than obtained for the cholesterol molecule ($D_{\|}=4.17\times10^{8}\,s^{-1}$).[97] This is perhaps expected due to the larger effective radius of the cholesterol compared to the phospholipid acyl segments, together with the lack of significant internal degrees of freedom of the rigid sterol ring system. The above conclusion seems to be in contrast with the result of Weisz *et al.*,[9] who have concluded that the cholesterol axial rotation is faster than that of phospholipids by about an order of magnitude. On the other hand, the off-axial rotational diffusion coefficient for phospholipids, although not very well determined from the fits, is smaller by more than a factor of 20, i.e., $D_{\perp}=0.399\times10^{6}\,s^{-1}$ versus $8.33\times10^{6}\,s^{-1}$. Molecular dynamics calculations[97,98] could probably shed additional light on the coupling of the dynamics of the phospholipids and cholesterol in the mixed bilayers. The above differences in diffusion coefficients and molecular ordering are clearly reflected in the magnitude of the observed relaxation rates of the phospholipids and cholesterol. For ^2H-labeled cholesterol in bilayers of DPPC at 30 °C, the spin-lattice relaxation rates are on the order of 150 to 500 s^{-1} and are close to the T_{1Z} minimum,[68,95] whereas the relaxation rates observed for the acyl chains of DMPC-d_{54}:cholesterol bilayers[8] are considerably smaller and range from 7 to 33 s^{-1}. This large difference is present even for the plateau region, which has the largest order parameter of $|S_{CD}|=0.42$.

In closing, it is perhaps worthwhile to emphasize that the present study comprises an important test of current models for the nuclear spin relaxation in lipid bilayers, involving extension of the range of their validity. Moreover, it represents one of the first examples in which the rotational dynamics of two interacting components in a mixed bilayer system have been comparatively analyzed in detail. As a rule, the ^2H NMR relaxation data as a function of frequency and sample orientation are successfully described for the acyl chains of both pure DMPC bilayers[59] and bilayers containing

cholesterol (this work) in terms of a composite membrane deformation model. The model yields an expression for the spectral densities in closed form, and allows one to obtain quantitative information about the bilayer. The results suggest the ^{2}H NMR relaxation of cholesterol-containing bilayers in the MHz regime is governed predominantly by noncollective molecular reorientations of the phospholipids and cholesterol, and less significantly by small-amplitude collective deformations of the membrane interior. The phospholipid molecules experience a somewhat higher axial mobility than in pure bilayers, e.g., arising from a reduction in the degrees of freedom due to chain entanglement, and have a greater axial mobility than the rigid cholesterol molecules. The internal configurational statistics of the chains are primarily manifested in the residual coupling tensor having variable components along the acyl chain, possibly due to alteration of the degree of chain entanglement as a result of interactions between the phospholipid and cholesterol molecules. Future work can test and extend the above framework by conducting relaxation studies of both the phospholipid and cholesterol constituents of the mixed bilayers over a broader range of frequencies. For instance, field-cycling techniques as pioneered by Noack[57] can be used for the lower frequencies, where slower collective motions are expected to be important. Likewise continued advancements in superconducting magnet technology allow access to increasingly higher frequencies that are indicative of faster molecular and segmental reorientations. These data can be more extensively modeled in the future using molecular mechanics computer simulations.[97–100] Finally, the approach could be extended to studies of membrane lipid:peptide interactions and protein:lipid interactions, including their dynamical coupling in relation to biological functions.

ACKNOWLEDGMENTS

Work supported by grants from the U.S. National Institutes of Health, the U.S. National Science Foundation, the Swedish Natural Science Research Council, and by an N.I.H. Postdoctoral Fellowship (T.M.A.).

[1] M. Bloom, C. Morrison, E. Sternin, and J. L. Thewalt, in *Pulsed Magnetic Resonance: NMR, ESR, and Optics. A Recognition of E. L. Hahn*, edited by D. M. S. Bagguley (Clarendon, Oxford, 1992), pp. 274–316.
[2] M. F. Brown, in *Biological Membranes. A Molecular Perspective from Computation and Experiment*, edited by K. M. Merz and B. Roux (Birkhäuser, Boston, 1996), pp. 175–252.
[3] R. A. Haberkorn, R. G. Griffin, M. D. Meadows, and E. Oldfield, J. Am. Chem. Soc. **99**, 7353 (1977).
[4] J. R. Brainard and A. Szabo, Biochemistry **20**, 4618 (1981).
[5] M. G. Taylor, T. Akiyama, and I. C. P. Smith, Chem. Phys. Lipids **29**, 327 (1981).
[6] E. J. Dufourc, E. J. Parish, S. Chitrakorn, and I. C. P. Smith, Biochemistry **23**, 6062 (1984).
[7] M. Bloom and O. G. Mouritsen, Can. J. Chem. **66**, 706 (1988).
[8] T. P. Trouard, T. M. Alam, J. Zajicek, and M. F. Brown, Chem. Phys. Lett. **189**, 67 (1992).
[9] K. Weisz, G. Gröbner, C. Mayer, J. Stohrer, and G. Kothe, Biochemistry **31**, 1100 (1992).
[10] C. Morrison and M. Bloom, J. Chem. Phys. **101**, 749 (1994).
[11] M. Bloom, E. Evans, and O. G. Mouritsen, Q. Rev. Biophys. **24**, 293 (1991).
[12] J. D. Pearlman, J. Zajicek, M. B. Merickel, C. S. Carman, C. R. Ayers, J. R. Brookeman, and M. F. Brown, Magn. Reson. Med. **7**, 262 (1988).
[13] B. J. Litman, O. Kalisky, and M. Ottolenghi, Biochemistry **20**, 631 (1981).
[14] D. C. Mitchell, M. Straume, J. L. Miller, and B. J. Litman, Biochemistry **29**, 9143 (1990).
[15] W. L. Hubbell and H. M. McConnell, J. Am. Chem. Soc. **93**, 314 (1971).
[16] M. F. Brown and J. Seelig, Biochemistry **17**, 381 (1978).
[17] D. J. Recktenwald and H. M. McConnell, Biochemistry **20**, 4505 (1981).
[18] M. Rance, K. R. Jeffrey, A. P. Tulloch, and K. W. Butler, Biochim. Biophys. Acta **688**, 191 (1982).
[19] F. T. Presti, in *Membrane Fluidity in Biology*, edited by R. E. Aloia and J. M. Boggs (Academic, 1985), Vol. 4, pp. 97–146.
[20] M. R. Vist and J. H. Davis, Biochemistry **29**, 451 (1990).
[21] Y.-K. Shin, J. K. Moscicki, and J. H. Freed, Biophys. J. **57**, 445 (1990).
[22] P. L. Yeagle, A. D. Albert, K. Boesze-Battaglia, J. Young, and J. Frye, Biophys. J. **57**, 413 (1990).
[23] J. H. Ipsen, G. Karlström, O. G. Mouritsen, H. Wennerström, and M. J. Zuckermann, Biochim. Biophys. Acta **905**, 162 (1987).
[24] G. W. Stockton and I. C. P. Smith, Chem. Phys. Lipids **17**, 251 (1976).
[25] E. Oldfield, M. Meadows, D. Rice, and R. Jacobs, Biochemistry **17**, 2727 (1978).
[26] A. Blume, Biochemistry **21**, 6230 (1982).
[27] F. T. Presti and S. I. Chan, Biochemistry **21**, 3821 (1982).
[28] M. Lafleur, P. R. Cullis, and M. Bloom, Eur. Biophys. J. **19**, 55 (1990).
[29] M. Jansson, R. L. Thurmond, J. A. Barry, and M. F. Brown, J. Phys. Chem. **96**, 9532 (1992).
[30] J. A. Barry and K. Gawrisch, Biochemistry **34**, 8852 (1995).
[31] H. Lecuyer and D. G. Dervichian, J. Mol. Biol. **45**, 39 (1969).
[32] T. J. McIntosh, Biochim. Biophys. Acta **513**, 43 (1978).
[33] J. H. Ipsen, O. G. Mouritsen, and M. Bloom, Biophys. J. **57**, 405 (1990).
[34] D. Needham, T. J. McIntosh, and E. Evans, Biochemistry **27**, 4668 (1988).
[35] H. P. Duwe and E. Sackmann, Physica A **163**, 410 (1990).
[36] R. A. Demel, W. S. M. Guerts Van Kessel, and L. L. M. Van Deenen, Biochim. Biophys. Acta **266**, 26 (1972).
[37] J. L. R. Rubenstein, B. A. Smith, and H. M. McConnell, Proc. Natl. Acad. Sci. USA **76**, 15 (1979).
[38] A. L. Kuo and C. G. Wade, Biochemistry **18**, 2300 (1979).
[39] J. Owicki and H. M. McConnell, Biophys. J. **30**, 383 (1980).
[40] G. Lindblom, L. B-Å Johansson, and G. Arvidson, Biochemistry **20**, 2204 (1981).
[41] M. R. Alecio, D. E. Golan, W. R. Veatch, and R. R. Rando, Proc. Natl. Acad. Sci. USA **79**, 5171 (1982).
[42] H. Kutchai, L. H. Chandler, and G. B. Zavoico, Biochim. Biophys. Acta **736**, 137 (1983).
[43] G. Lindblom and G. Orädd, Prog. Nucl. Magn. Reson. Spectrosc. **26**, 483 (1994).
[44] M. F. Brown, J. Magn. Reson. **35**, 203 (1979).
[45] M. F. Brown, J. Seelig, and U. Häberlen, J. Chem. Phys. **70**, 5045 (1979).
[46] D. A. Torchia and A. Szabo, J. Magn. Reson. **49**, 107 (1982).
[47] M. F. Brown, J. Chem. Phys. **77**, 1576 (1982).
[48] A. Szabo, J. Chem. Phys. **81**, 150 (1984).
[49] B. Halle, J. Phys. Chem. **95**, 6724 (1991).
[50] J. A. Marqusee, M. Warner, and K. A. Dill, J. Chem. Phys. **81**, 6404 (1984).
[51] B. Halle and S. Gustafsson, Phys. Rev. E **56**, 690 (1997).
[52] A. A. Nevzorov and M. F. Brown, J. Chem. Phys. **107**, 10288 (1997).
[53] G. Moro and J. H. Freed, J. Chem. Phys. **74**, 3757 (1981).
[54] K. Müller, P. Meier, and G. Kothe, Prog. Nucl. Magn. Reson. Spectrosc. **17**, 211 (1985).
[55] D. J. Schneider and J. H. Freed, Adv. Chem. Phys. **73**, 387 (1989).
[56] P. Meier, E. Ohmes, and G. Kothe, J. Chem. Phys. **85**, 3598 (1986).
[57] E. Rommel, F. Noack, P. Meier, and G. Kothe, J. Phys. Chem. **92**, 2981 (1988).
[58] J. Stohrer, G. Gröbner, D. Reimer, K. Weisz, C. Mayer, and G. Kothe, J. Chem. Phys. **95**, 672 (1991).
[59] A. A. Nevzorov, T. P. Trouard, and M. F. Brown, Phys. Rev. E **58**, 2259 (1998).
[60] R. Ghosh and J. Seelig, Biochim. Biophys. Acta **691**, 151 (1982).
[61] H. C. Jarrell, P. A. Jovall, J. B. Giziewicz, L. A. Turner, and I. C. P. Smith, Biochemistry **26**, 1805 (1987).
[62] C. Mayer, G. Gröbner, K. Müller, K. Weisz, and G. Kothe, Chem. Phys. Lett. **165**, 155 (1990).
[63] J. B. Speyer, R. T. Weber, S. K. Das Gupta, and R. G. Griffin, Biochemistry **28**, 9569 (1989).

[64] H. C. Jarrell, I. C. P. Smith, P. A. Jovall, H. H. Mantsch, and D. J. Siminovitch, J. Chem. Phys. **88**, 1260 (1988).
[65] T. P. Trouard, T. M. Alam, and M. F. Brown, J. Chem. Phys. **101**, 5229 (1994).
[66] D. J. Siminovitch, M. J. Ruocco, E. T. Olejniczak, S. K. Das Gupta, and R. G. Griffin, Biophys. J. **54**, 373 (1988).
[67] J.-M. Bonmatin, I. C. P. Smith, H. C. Jarrell, and D. J. Siminovitch, J. Am. Chem. Soc. **110**, 8693 (1988).
[68] J.-M. Bonmatin, I. C. P. Smith, H. C. Jarrell, and D. J. Siminovitch, J. Am. Chem. Soc. **112**, 1697 (1990).
[69] A. Abragam, *The Principles of Nuclear Magnetism* (Oxford University Press, London, 1961).
[70] H. W. Spiess, in *NMR Basic Principles and Progress*, edited by P. Diehl, E. Fluck, and R. Kosfeld (Springer-Verlag, Heidelberg, 1978), Vol. 15, pp. 55–214.
[71] M. F. Brown and S. I. Chan, in *Encyclopedia of Nuclear Magnetic Resonance*, edited by D. M. Grant and R. K. Harris (Wiley, New York, 1996), Vol. 2, pp. 871–885.
[72] Abbreviations used: 2D, two dimensional; 3D, three dimensional; DMPC, 1,2-dimyristoyl-s*n*-glycero-3-phosphocholine; DMPC-d_{54}, 1,2-diperdeuteriomyristoyl-s*n*-glycero-3-phosphocholine; DPPC, 1,2-dipalmitoyl-s*n*-glycero-3-phosphocholine; EFG, electric field gradient; EPR, electron paramagnetic resonance; NMR, nuclear magnetic resonance; ODF, order-director fluctuations; PAS, principal axis system.
[73] D. M. Brink and G. R. Satchler, *Angular Momentum* (Oxford University Press, London, 1968).
[74] T. M. Barbara, R. R. Vold, and R. L. Vold, J. Chem. Phys. **79**, 6338 (1983).
[75] M. F. Brown and O. Söderman, Chem. Phys. Lett. **167**, 158 (1990).
[76] P. L. Nordio and U. Segre, in *The Molecular Physics of Liquid Crystals*, edited by G. R. Luckhurst and G. W. Gray (Academic, New York, 1979), pp. 411–426.
[77] P. Ukleja, J. Pirs, and J. W. Doane, Phys. Rev. A **14**, 414 (1976).
[78] P. Pincus, Solid State Commun. **7**, 415 (1969).
[79] R. Y. Dong, *Nuclear Magnetic Resonance of Liquid Crystals* (Springer-Verlag, New York, 1994).
[80] J. H. Freed, J. Chem. Phys. **66**, 4183 (1977).
[81] R. R. Vold, in *Nuclear Magnetic Resonance Probes of Molecular Dynamics*, edited by R. Tycko (Kluwer, Dordrecht, 1994), Vol. 8, pp. 27–112.
[82] J. T. Mason, A. V. Broccoli, and C. H. Huang, Anal. Biochem. **113**, 96 (1981).
[83] S. W. Dodd, M.S. Thesis, University of Virginia, 1987.
[84] T. P. Trouard, Ph.D. Dissertation, University of Virginia, 1992.
[85] R. R. Vold and G. Bodenhausen, J. Magn. Reson. **39**, 363 (1980).
[86] S. Wimperis, J. Magn. Reson. **86**, 46 (1990).
[87] G. L. Hoatson, J. Magn. Reson. **94**, 152 (1991).
[88] K. R. Jeffrey, Bull. Magn. Reson. **3**, 69 (1981).
[89] H. U. Gally, A. Seelig, and J. Seelig, Hoppe-Seyler's Z. Physiol. Chem. **357**, 1447 (1976).
[90] G. D. Williams, J. M. Beach, S. W. Dodd, and M. F. Brown, J. Am. Chem. Soc. **107**, 6868 (1985).
[91] L. J. Korstanje, E. E. van Faassen, and Y. K. Levine, Biochim. Biophys. Acta **982**, 196 (1989).
[92] M. A. Davies, H. F. Schuster, J. W. Brauner, and R. Mendelsohn, Biochemistry **29**, 4368 (1990).
[93] R. Blinc, M. Luzar, M. Vilfan, and M. Burgar, J. Chem. Phys. **63**, 3445 (1975).
[94] B. A. Cornell and M. Keniry, Biochim. Biophys. Acta **732**, 705 (1983).
[95] E. J. Dufourc and I. C. P. Smith, Chem. Phys. Lipids **41**, 123 (1986).
[96] M. F. Brown, Mol. Phys. **71**, 903 (1990).
[97] H. E. Alper, D. Bassolino-Klimas, and T. R. Stouch, J. Chem. Phys. **99**, 5547 (1993).
[98] R. M. Venable, Y. Zhang, B. J. Hardy, and R. W. Pastor, Science **262**, 223 (1993).
[99] K. Tu, J. T. Douglas, and M. L. Klein, Biophys. J. **69**, 2558 (1995).
[100] S.-W. Chiu, M. Clark, V. Balaji, S. Subramaniam, H. L. Scott, and E. Jakobsson, Biophys. J. **69**, 1230 (1995).
[101] J. H. Davis, K. R. Jeffrey, M. Bloom, M. I. Valic, and T. P. Higgs, Chem. Phys. Lett. **44**, 390 (1976).
[102] P. R. Bevington, *Data Reduction and Error Analysis for the Physical Sciences* (McGraw-Hill, New York, 1969).